Josephson Flux Flow Oscillators; principles of operation and applications

Jesper Mygind*, Mogens R. Samuelsen

Department of Physics, B309, Technical University of Denmark, Lyngby Denmark.

Alexander S. Sobolev, Valery P. Koshelets

Institute of Radio Engineering and Electronics, RAS, Moscow, Russia

Work supported in part by the RFBR project 03-02-16748, INTAS project 01-0367, ISTC project 2445, the NATO Science for peace SfP 981415, Danish Natural Science Foundation, and the Hartmann Foundation.

Overview

The Superconducting Integrated Receiver (SIR)

SIS mixer, coupling to antenna and LO

Josephson oscillators, Flux Flow Oscillator (FFO), emitted power

I_B -V- I_{CL} curves, Fiske Steps (FS), Flux Flow Step, sine-Gordon eq.

The SIR in action. SRON and the TELIS project

FFO linewidth

FFO tunability, frequency and phase locking, PLL

Simple theory for FFO linewidth

- **Theory *long ideal* (“bare”) junction**
- **Magnetic field from bias current, short junction with coil**
- **Examples**
- **Measurements, the K-factor**

Conclusion and outlook

The

All-Superconducting Integrated Receiver (SIR)

is based on the

quasi-particle (SIS) mixer/detector

pumped by the Flux Flow Oscillator (FFO)

Micro-photograph of the SIR chip with antenna, SIS-mixer and phase-locked FFO

Chip size is 4 mm by 4 mm.

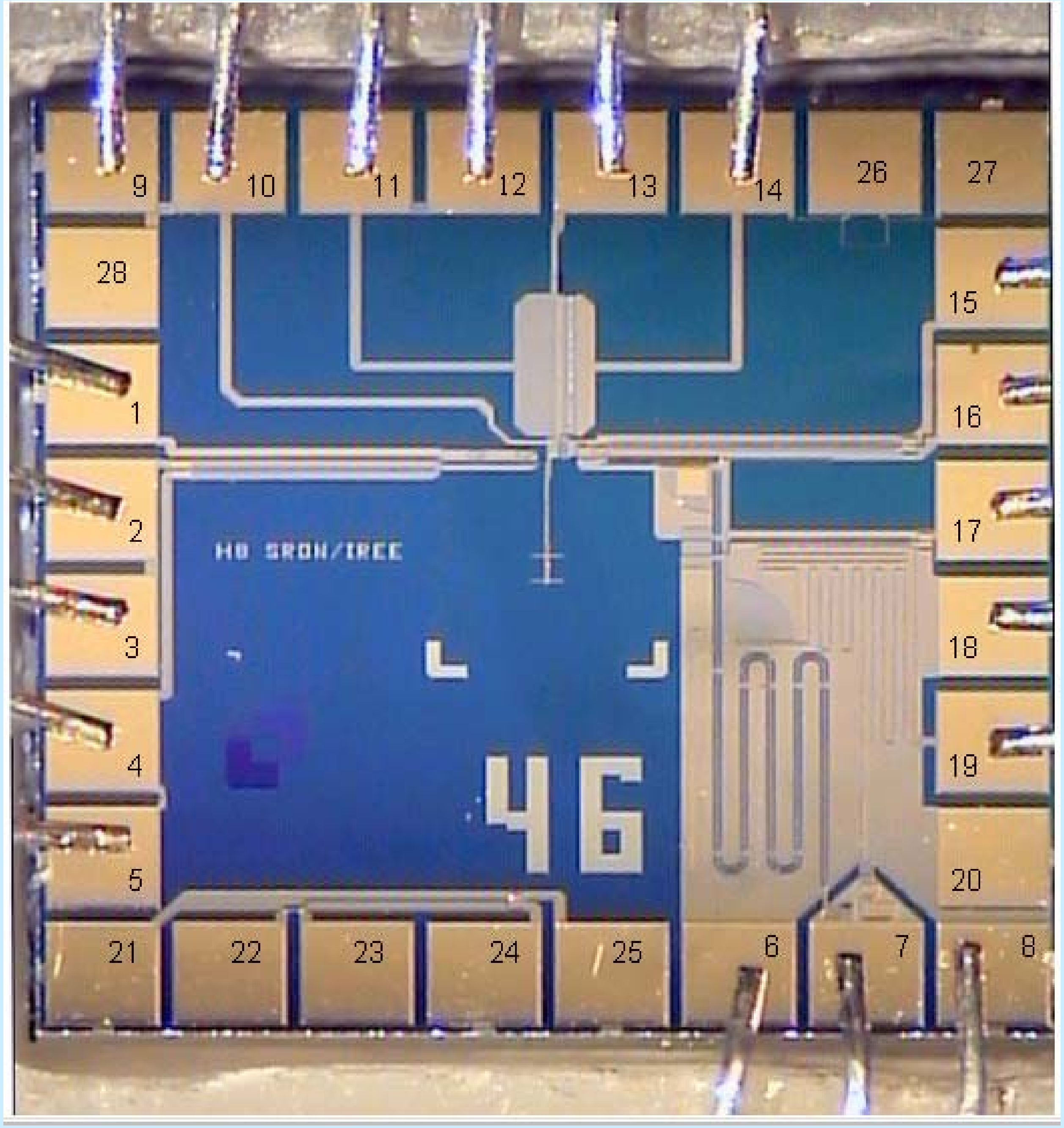

Blow-up of central part of SIR chip showing:

Double quarter-wave antenna

SIS mixer

LO (FFO) feeder

IF out & DC bias

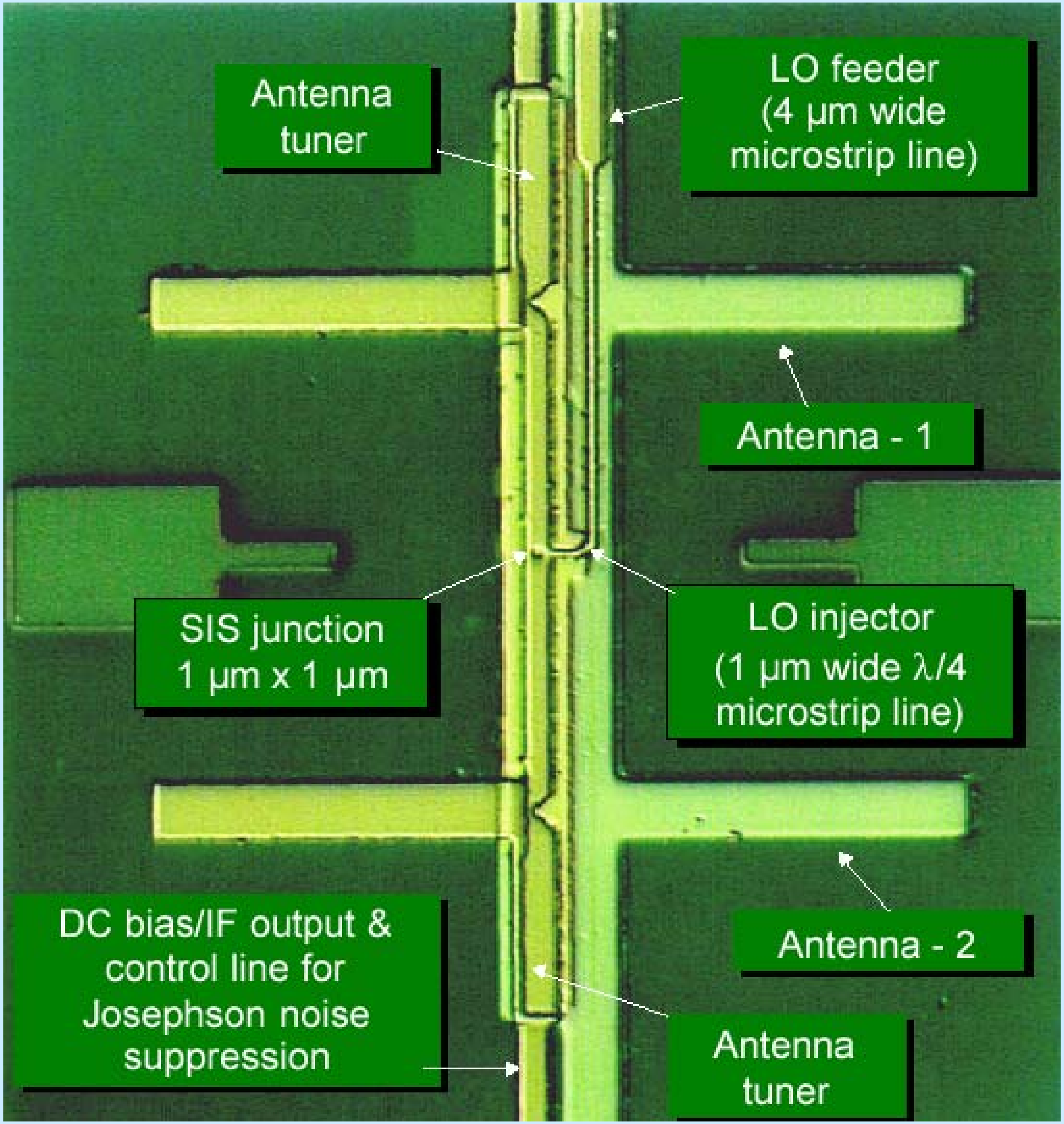

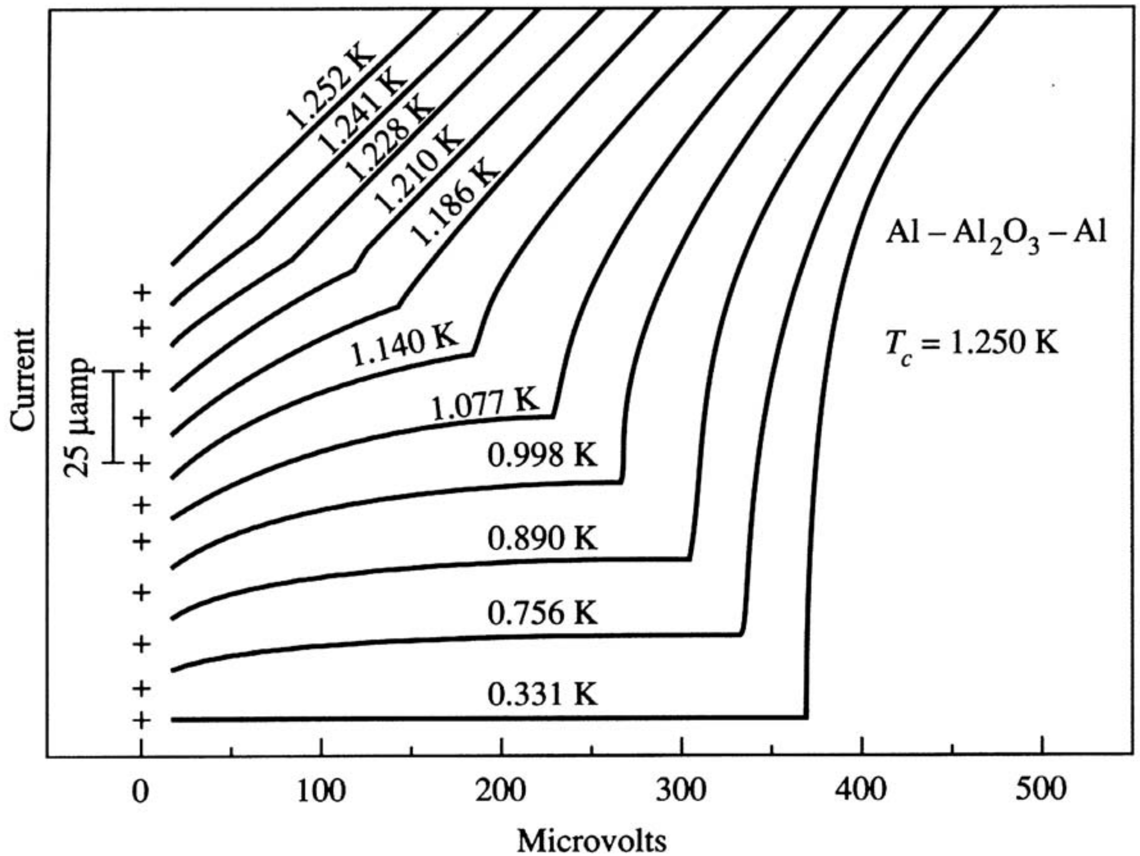

A sequence of current-voltage characteristics at various temperatures for a constant voltage source driving the junction. The curves are offset from zero for clarity. *Source: B. L. Blackford and R. H. March, "Temperature Dependence of the Energy Gap in Superconductivity A1-A1$_2$O$_3$-A1 Tunnel Junctions,"* Canadian Journal of Physics, *Vol. 46 (1968).*

DTU

DC I-V curve for **SIS junction**

Quasi-particle current vs. temperature shows also **Δ**(T)

Used in the SIS mixer and in many bolometric detectors

Josephson junction subjected to high frequency signals

SIS mixer pumped at 260, 350, 530 and 665 GHz

Arrows point at the first Shapiro steps (JVS) and the quasi-particle steps (photon assisted tunneling, PAT)

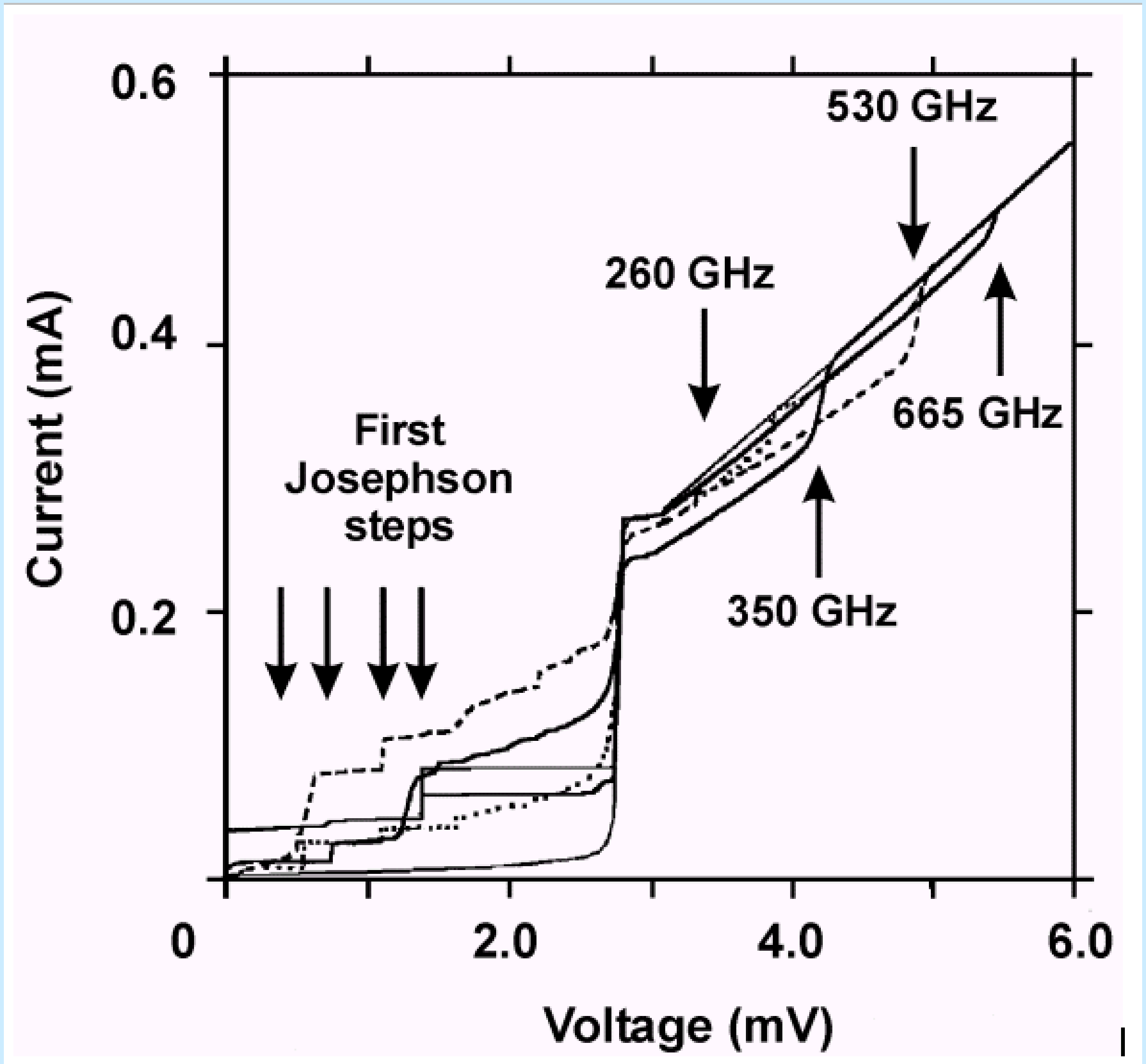

Replaceable Module of the 500 GHz

Imaging Array Superconducting Integrated Receiver

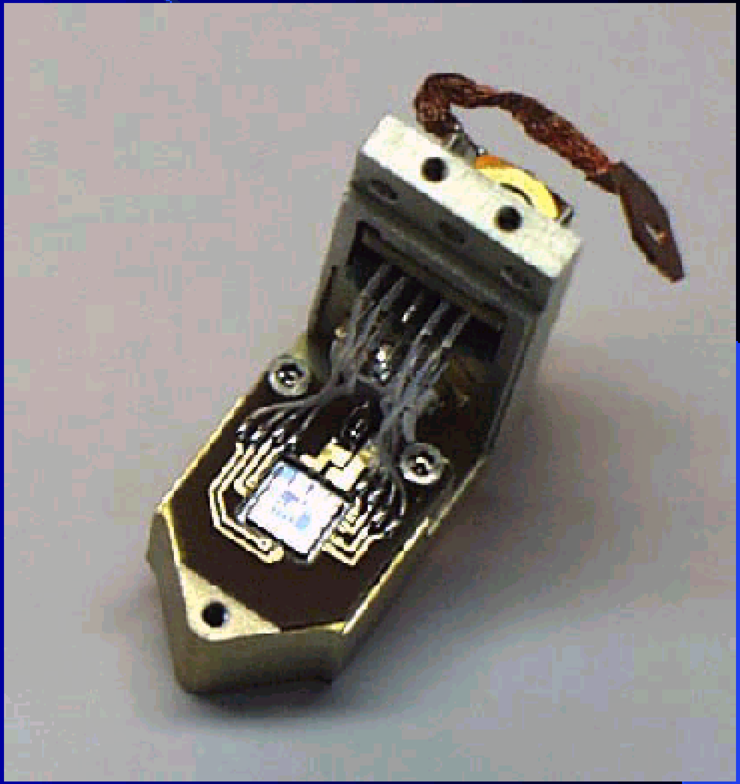

Nine-pixel Imaging Array Receiver Block.

Antenna-Lens Beam Pattern of the SIR at 625 GHz

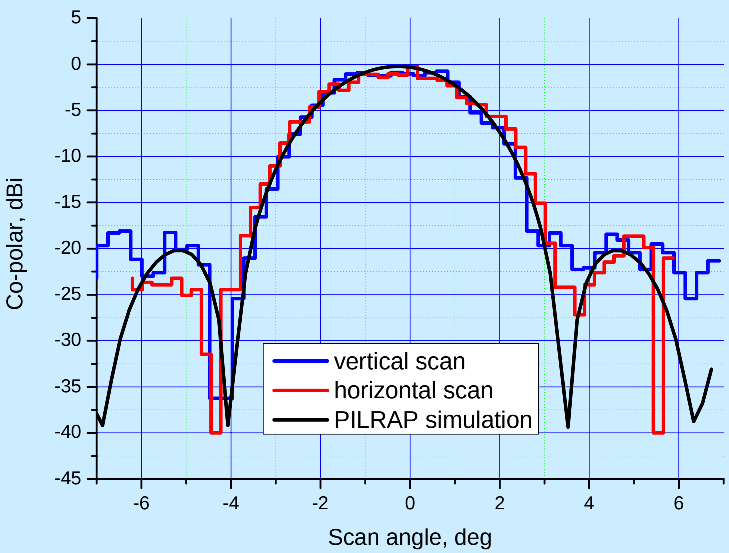

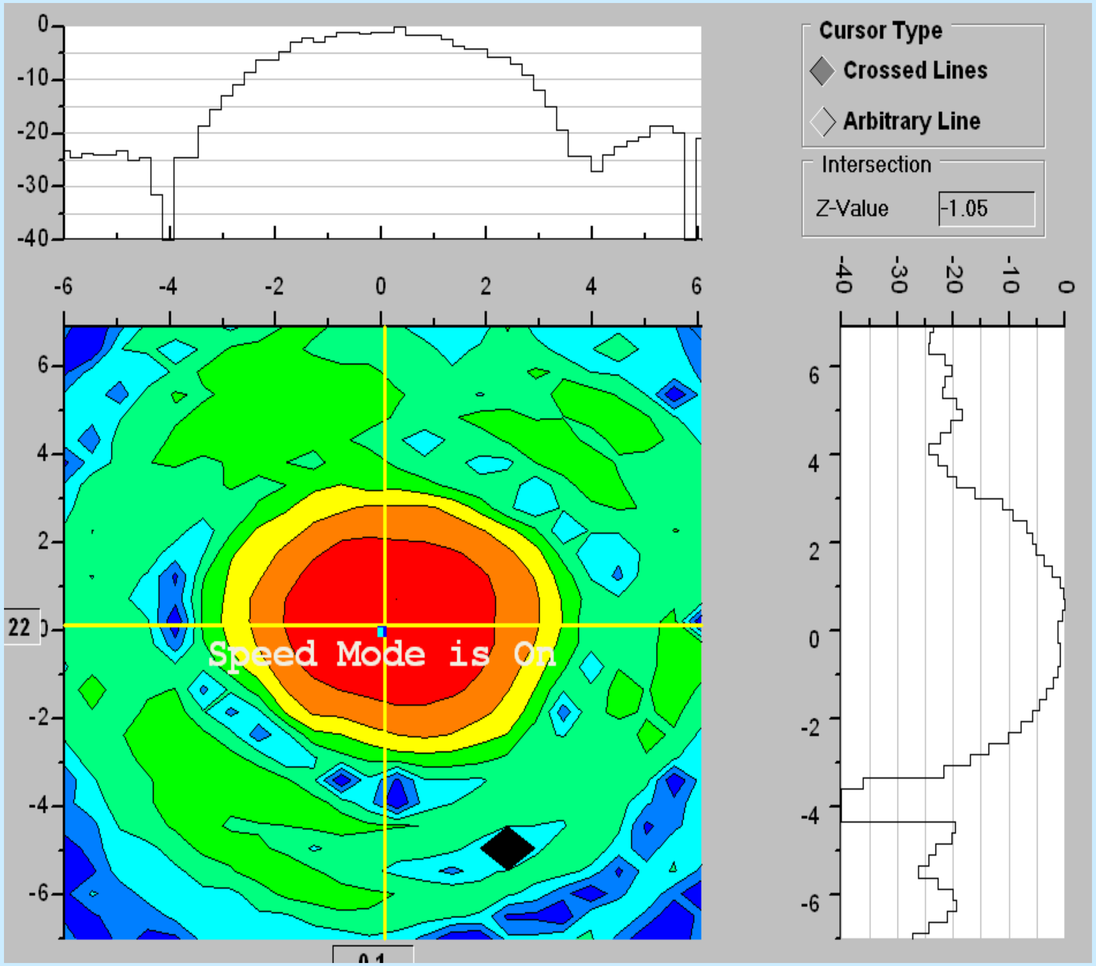

FFO-NN-2009

Sub-mm receiver with external LO (BWO)

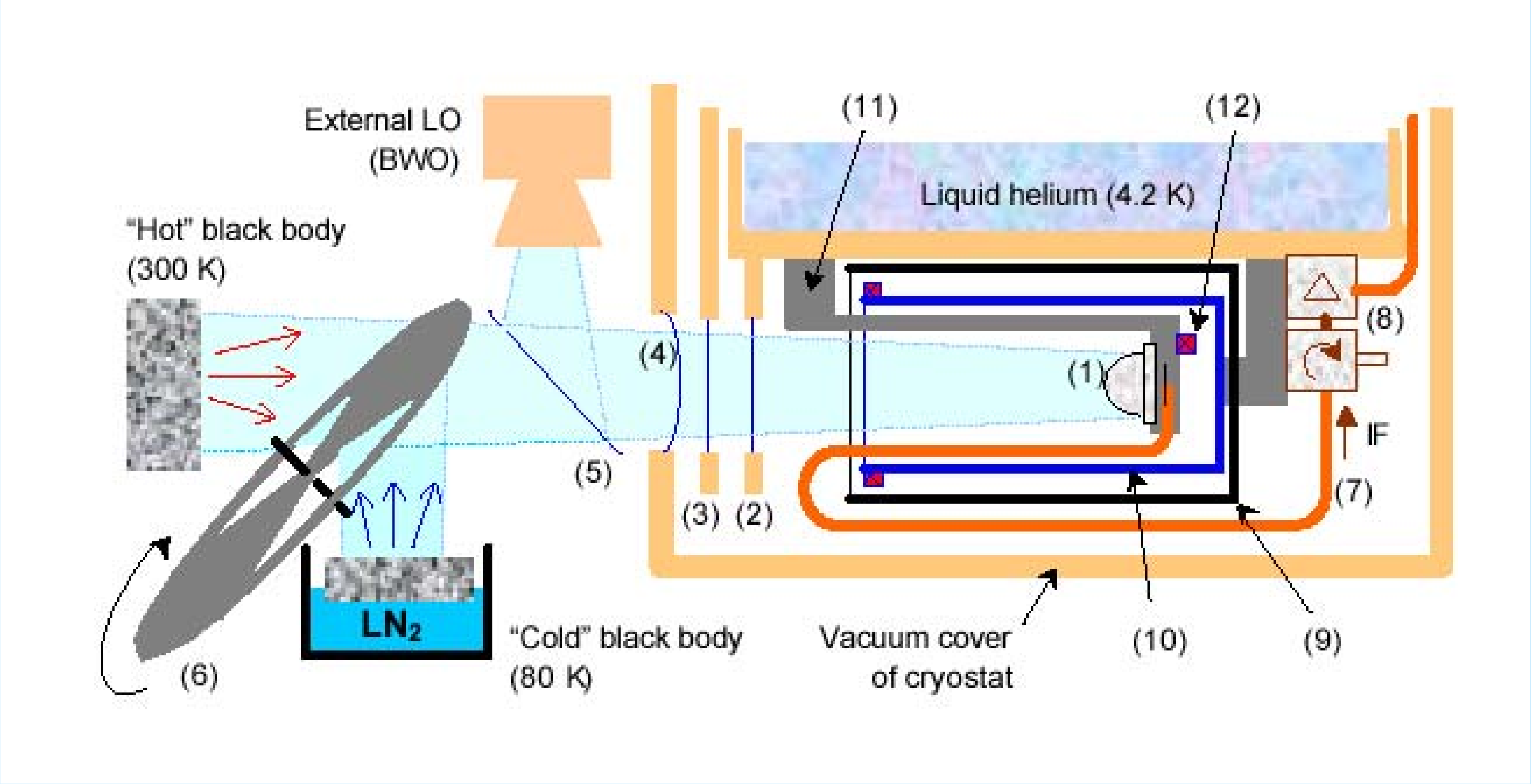

Noise Temperature of the **TErahertz LImb Sounder (TELIS)** SIR (DSB)

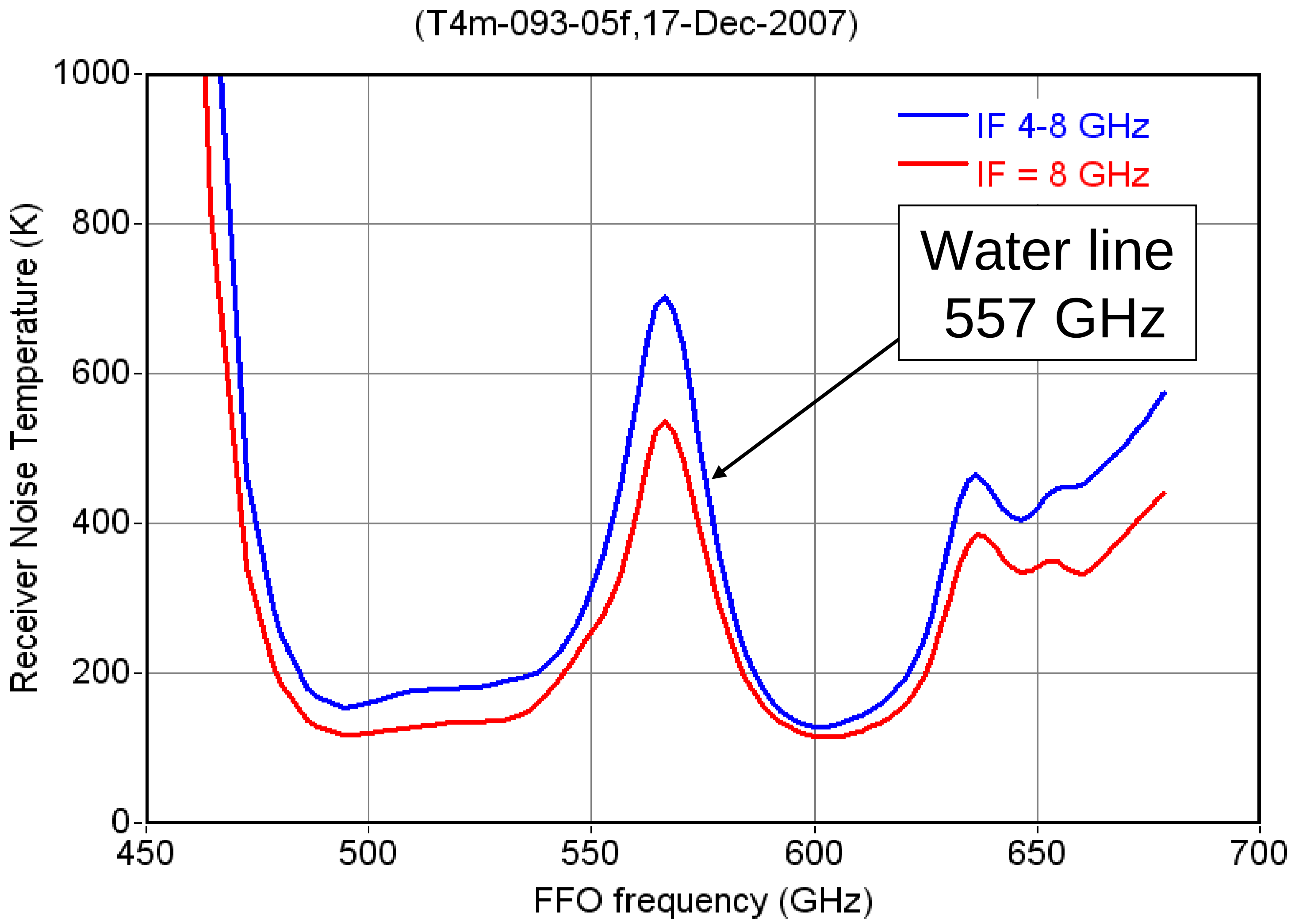

Josephson oscillators

Emitted power from mm and sub-millimeter oscillators

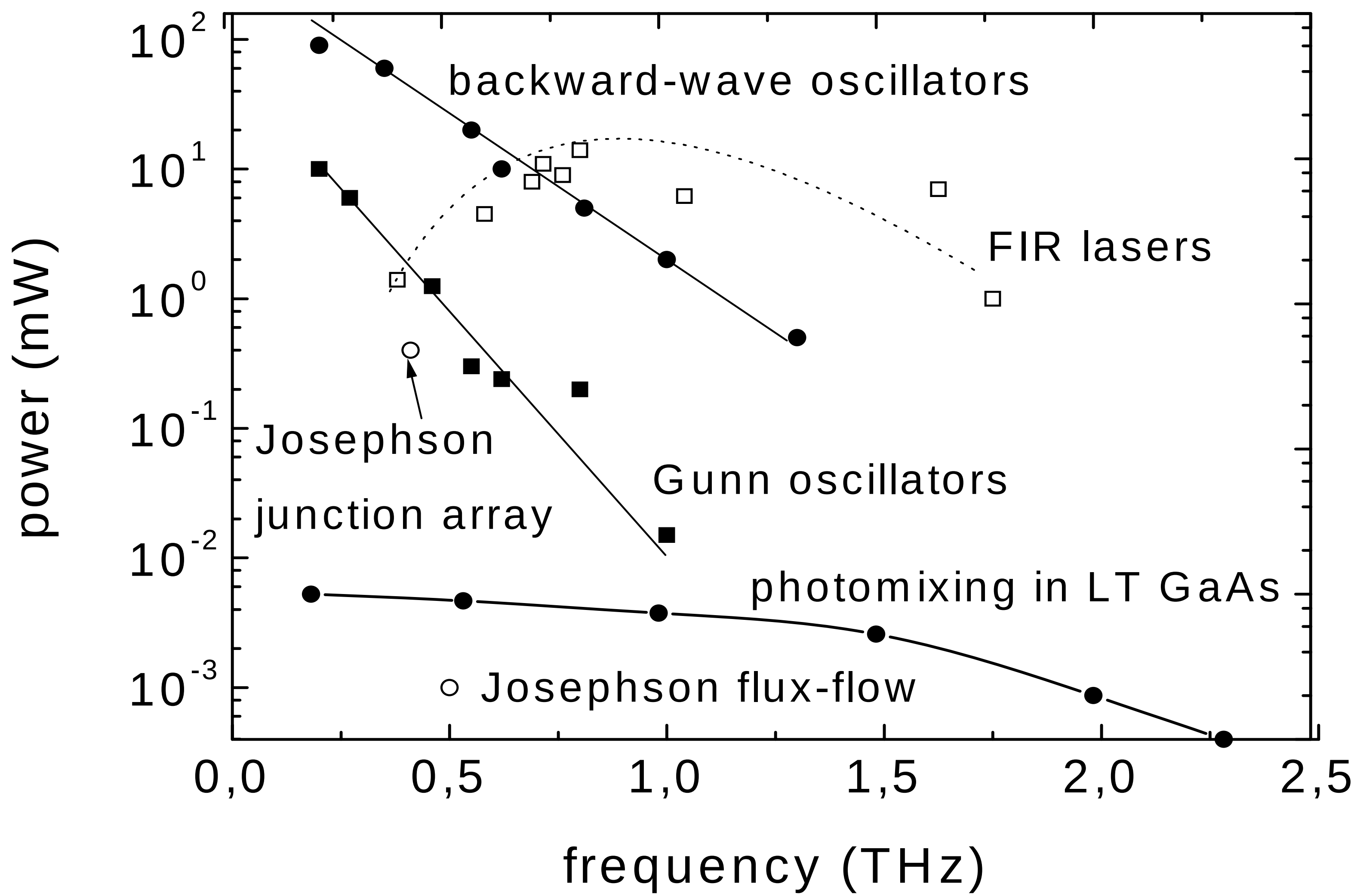

only a few microwatts needed on-chip!

Three types of Josephson junctions

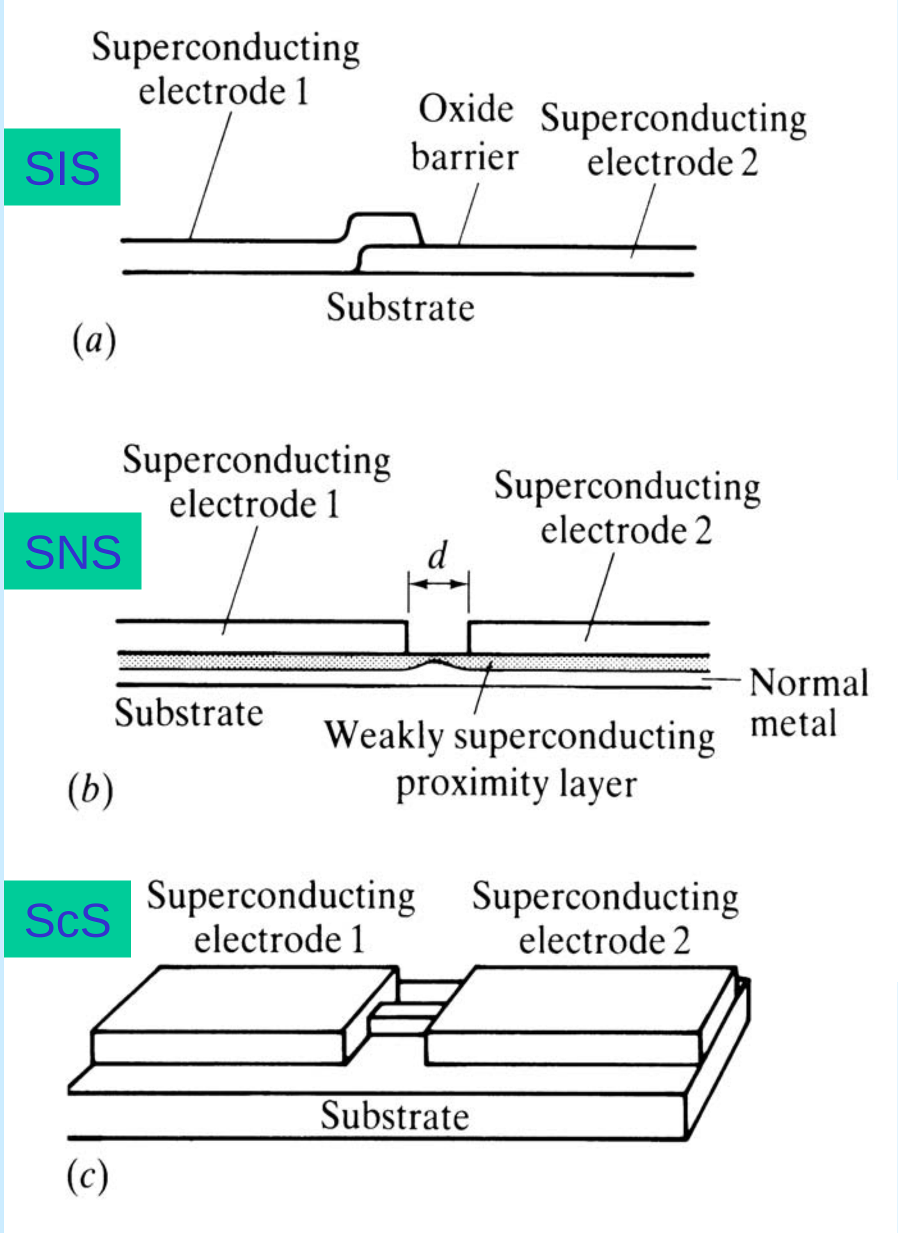

Josephson effect and equations

$$I = I_C \sin \varphi$$

$$\partial \varphi / \partial t = (2\pi/\Phi_0)V$$

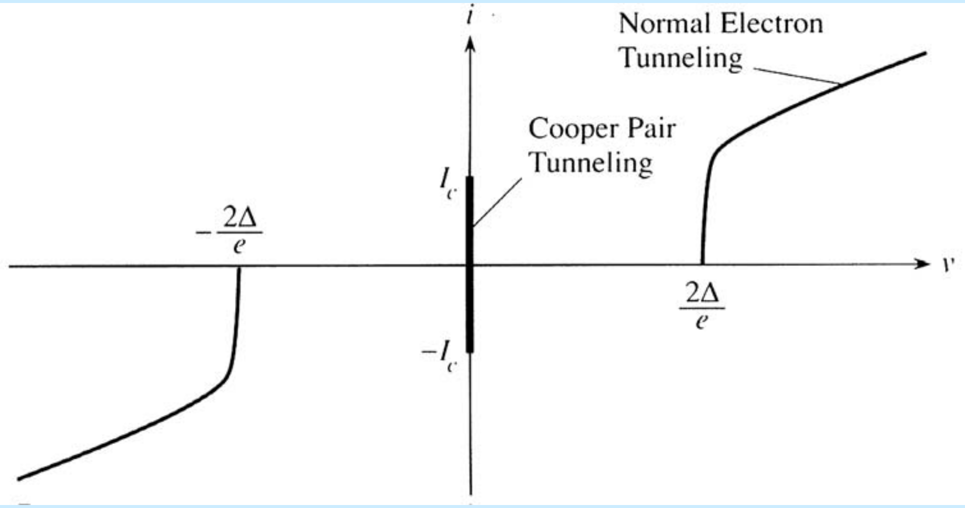

DC I-V curve for SIS junction (current biased, idealized)

Current biased resistively shunted junction (RSJ) model

(negligible capacitance)

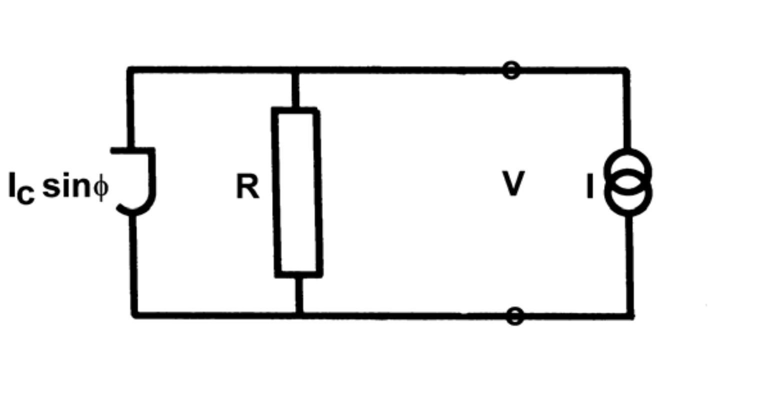

DC I-V curve

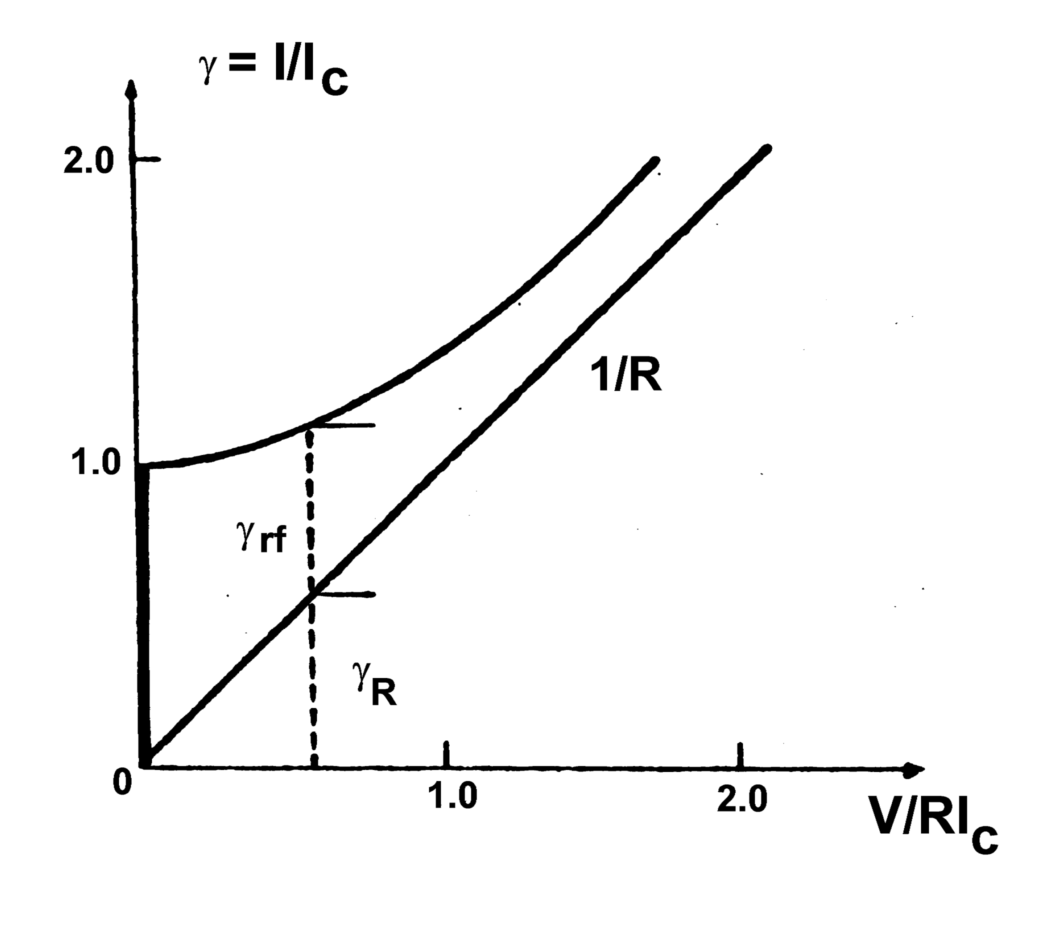

γ_{rf} ∝ available for rf
γ_R ∝ resistive loss

Power, linewidth and tunability

The long ($L >> \lambda_J$) Josephson tunnel junction

FFO: Viscous flow of magnetic quanta driven by a bias current and an applied magnetic field

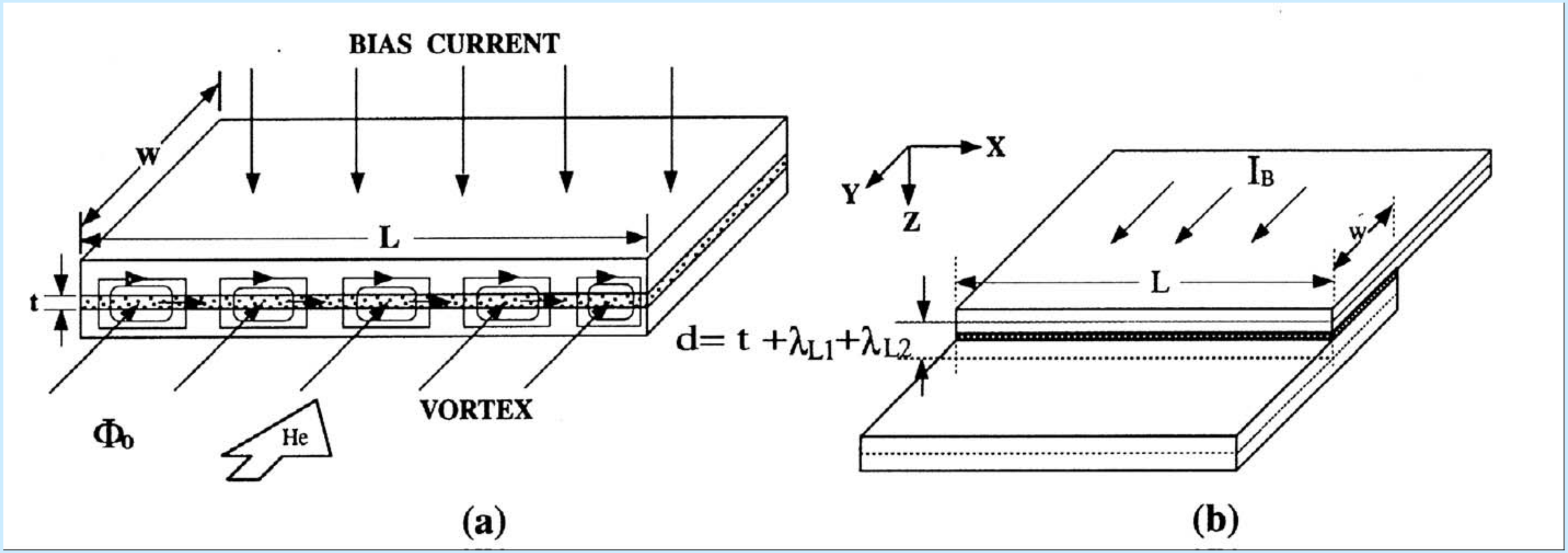

The resonant soliton oscillator, RSO, without applied magnetic field

Bare junction, long rectangular geometry

Modeled by the perturbed 1-D sine-Gordon equation

$$\phi_{xx} - \phi_{tt} = \sin\phi + \alpha\phi_t - \eta,$$

where the normalized *overlap* current through the junction is η and α is the normalized damping. Time t is normalized to the inverse maximum plasma frequency, ω_0, length x to the Josephson penetration length, λ_J, currents to the maximum critical current, I_c, and magnetic fields to $I_c\lambda_J$ which is half of the critical field, $H_c = 2I_c\lambda_J$, needed to force the first fluxon into the junction.

FFO

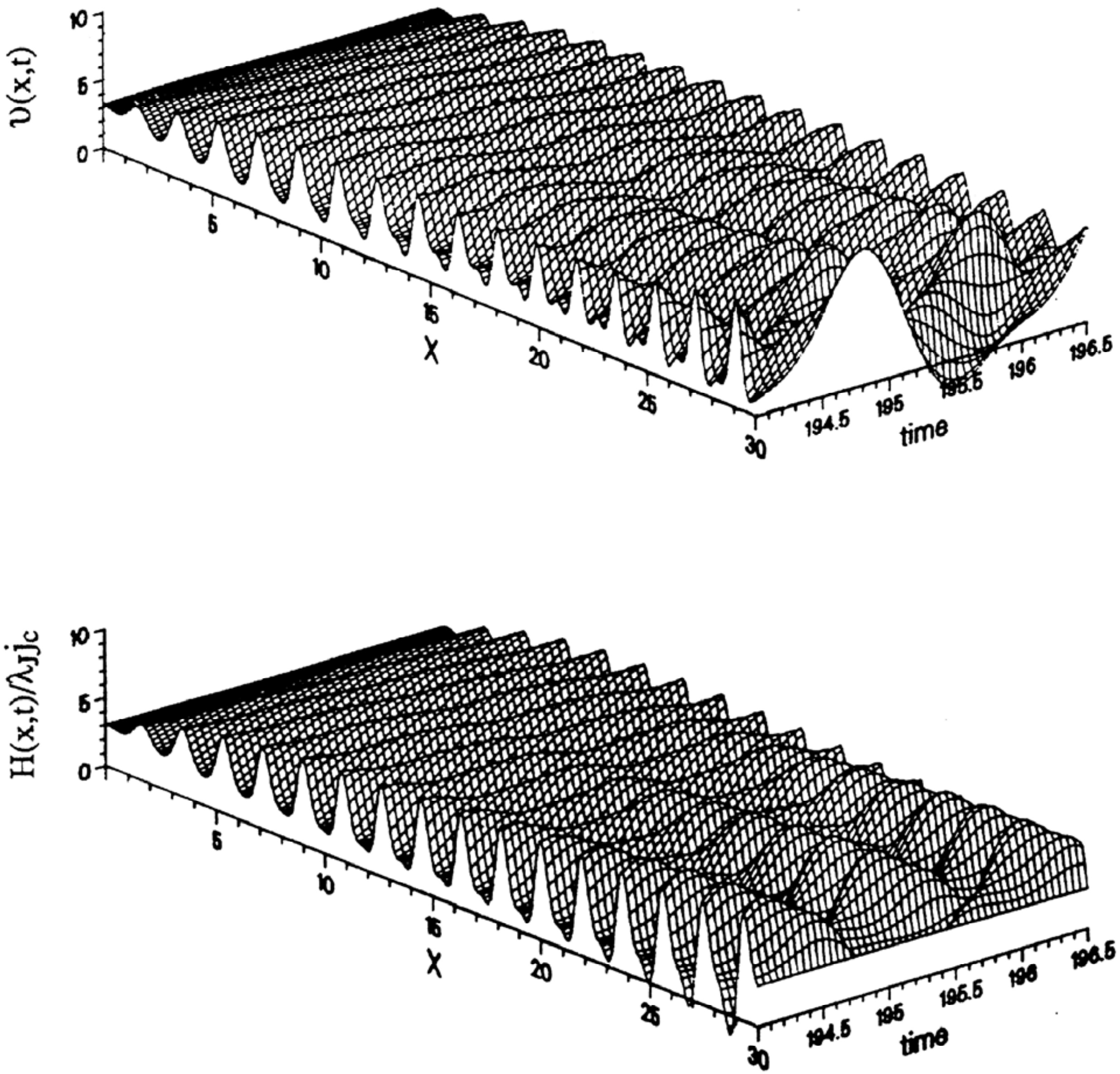

Numerical calculation of flux flow in long JJ (Y. Zhang)

Note: sinusoidal output voltage, low content of higher harmonics

Calculated DC I-V curve for FFO

Numerical simulation with normalized length = 15, normalized magnetic field = 6 and damping ***α*** = 0.1

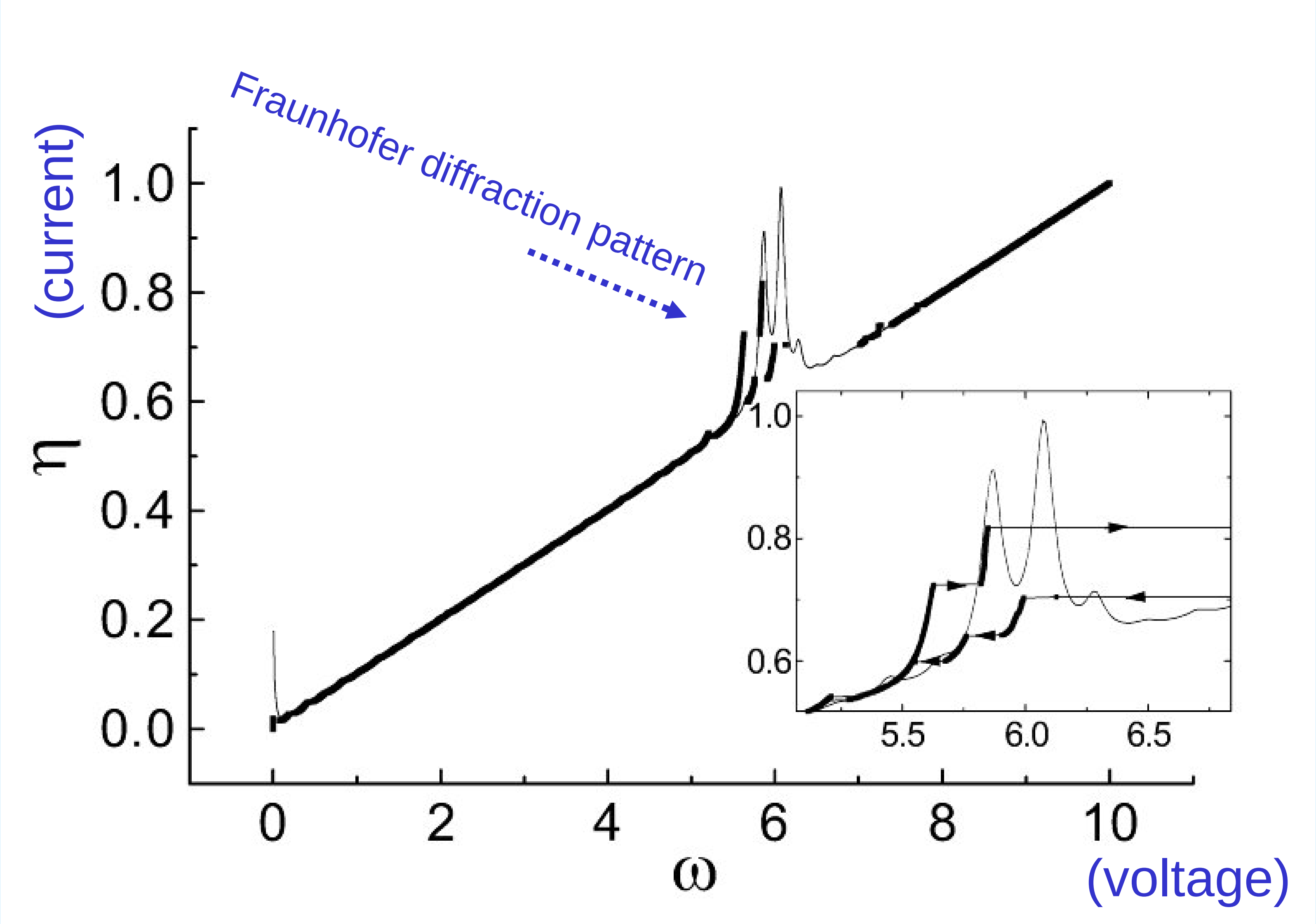

Set of IVCs for Nb-AlO_x-Nb FFO recorded for fixed control line current, I_{CL}, which is then incremented by $\Delta I_{CL} \approx 0.5$ mA before the next IVC is recorded.

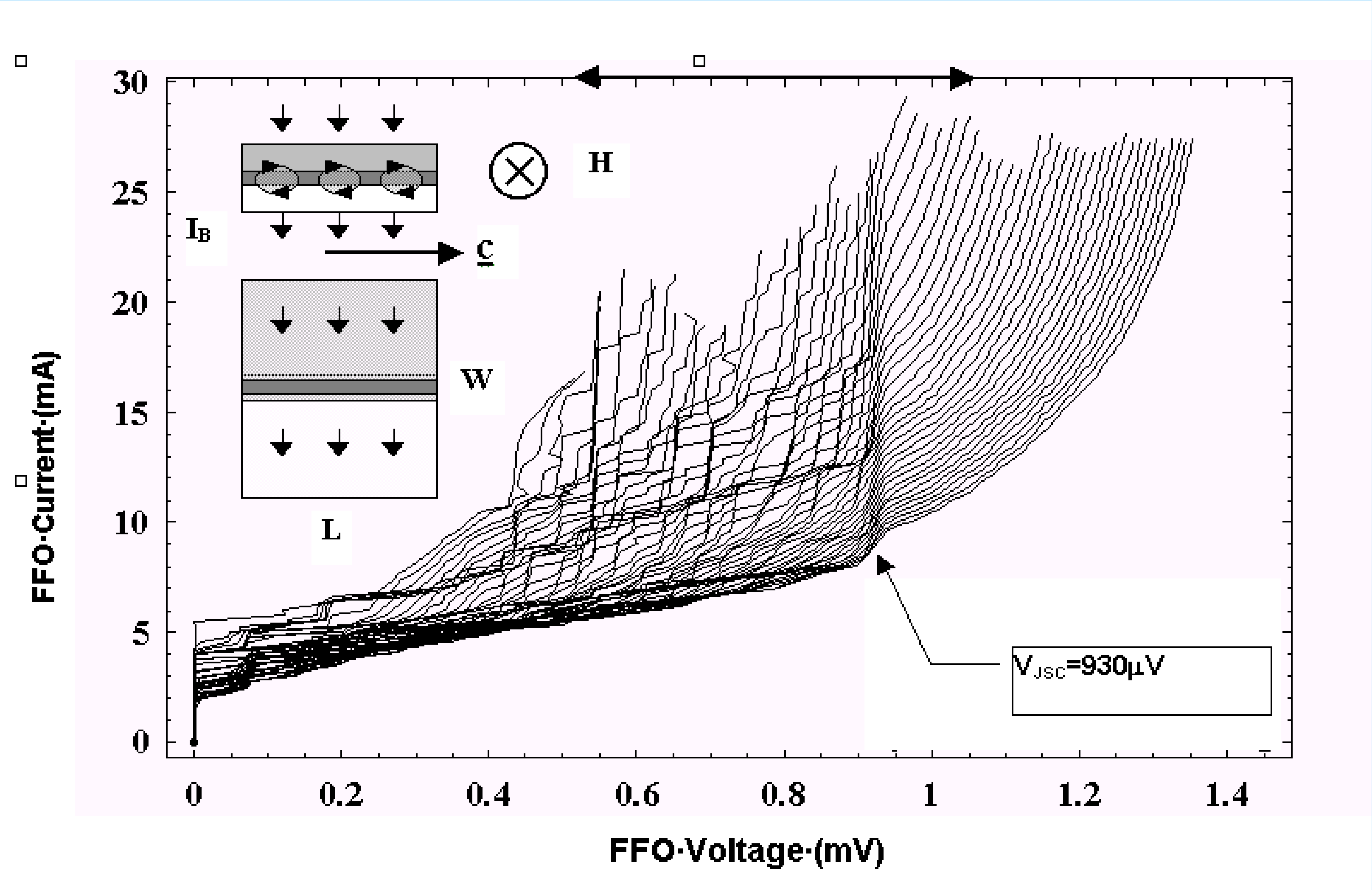

DC and RF properties are understood

MOST IMPORTANT IS TUNABILITY

The SIR in action

with

SRON, Netherlands Institute for Space Research

Heterodyne Receivers at SRON

- HIFI - Herschel Space Observatory
  – 480 to 1900 GHz SIS/HEB
- Atacama Large Millimeter Array (ALMA)
  – 650 GHz SIS
- Atacama Pathfinder Experiment (APEX)
  - 650 GHz / 810 GHz mixer array
- Terahertz Limb Sounder (TELIS)
  - 650 GHz Integrated Receiver
- HEB-QCL research up to 6 THz
- Space interferometer concept and Millimetron

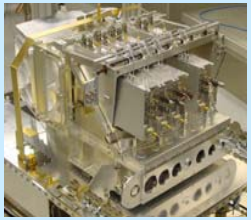
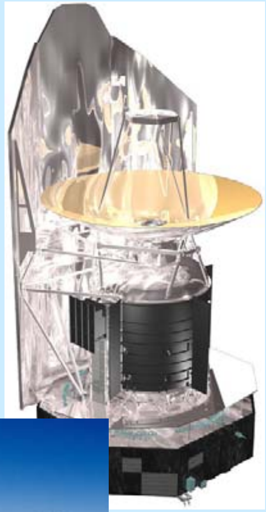



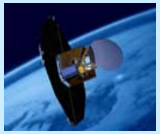
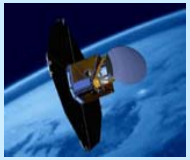
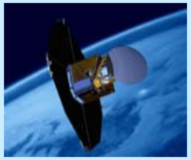
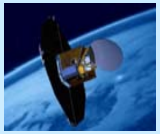
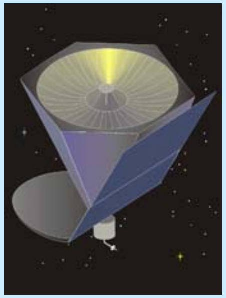
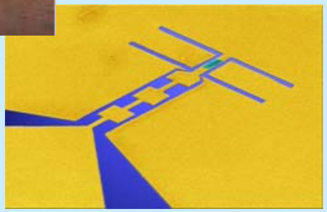
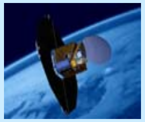
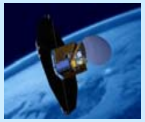

TELIS

- Acronym: TErahertz LImb Sounder
- Balloon instrument on board the MIPAS gondola, IMK Karlsruhe
- Three independent frequency channels, cryogenic heterodyne receivers:
  - 500 GHz by RAL
  - 500-650 GHz by SRON
  - 1.8 THz by DLR (PI)

Typical atmospheric spectrum

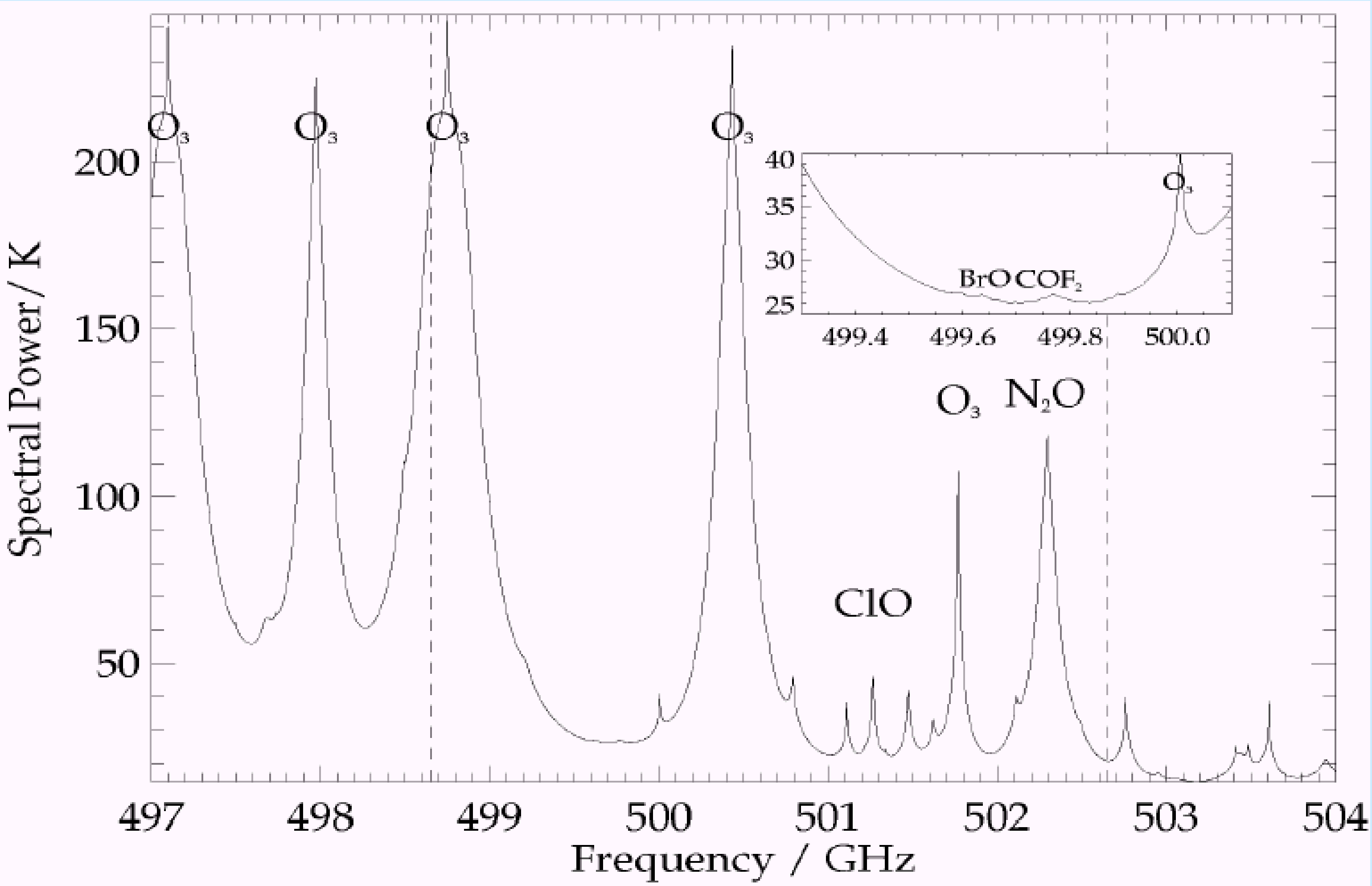

The SIR is a high resolution spectrometer

TELIS schematics

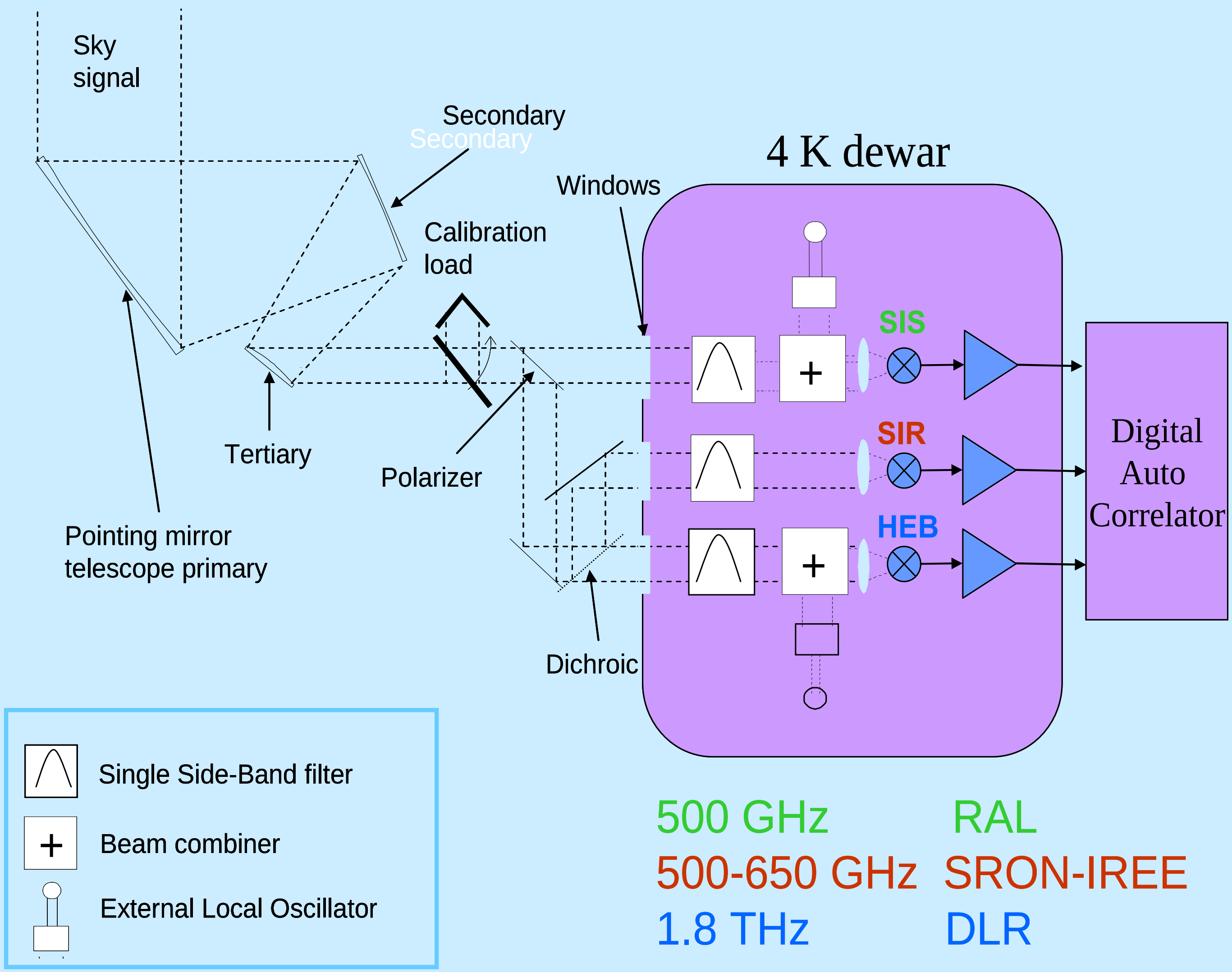

500 GHz RAL
500-650 GHz SRON-IREE
1.8 THz DLR

Photo of the T4m SIR chip

Silicon (Si);

$4 \times 4 \times 0.5\ mm^3$

Nb-AlOx-Nb or

Nb-AlN-NbN

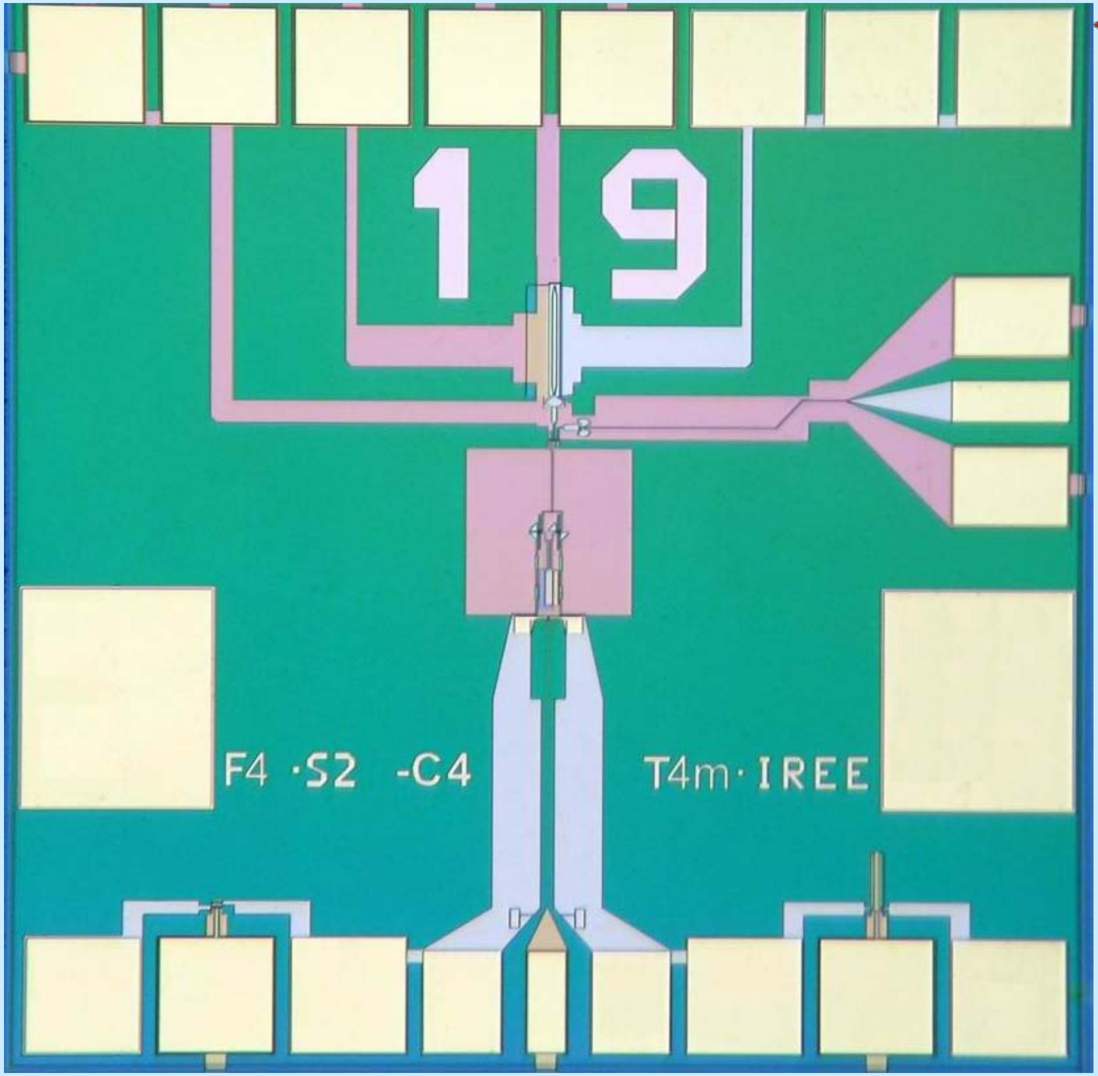

SIR Microcircuit for TELIS

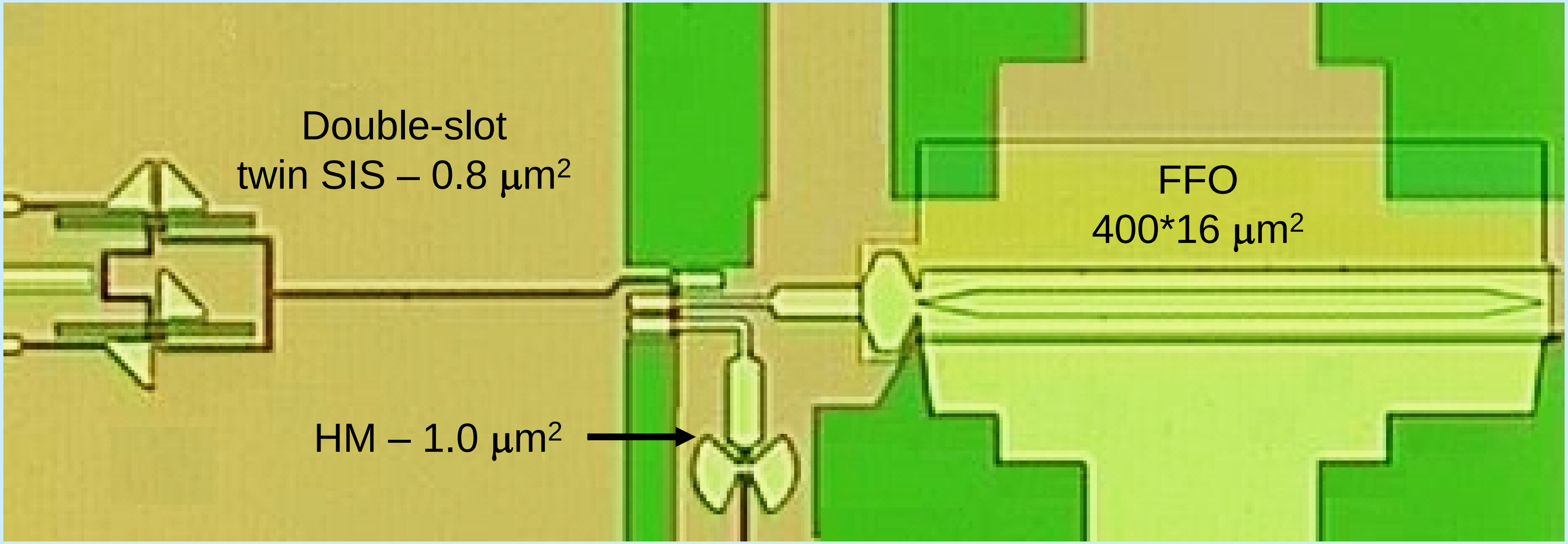

Nb-AlN-NbN or Nb-AlOx-Nb; Jc = 5 - 10 kA/cm²

Optionally: SIS – Jc = 8 kA/cm²; FFO + HM = 4 kA/cm²

Nb-AlN-NbN SIS pumped by FFO; FFO frequency tuning

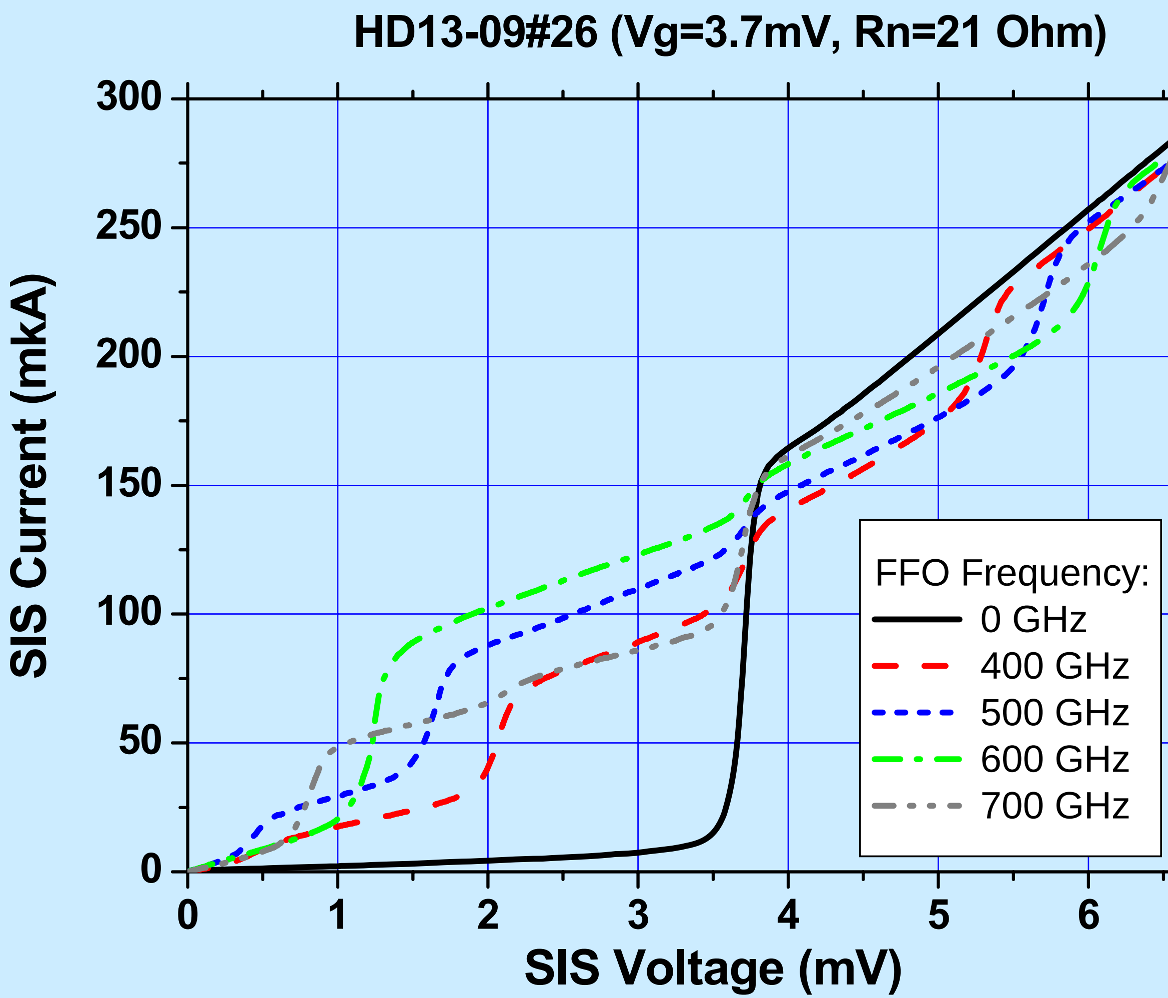

Nb-AlN-NbN SIR – new features

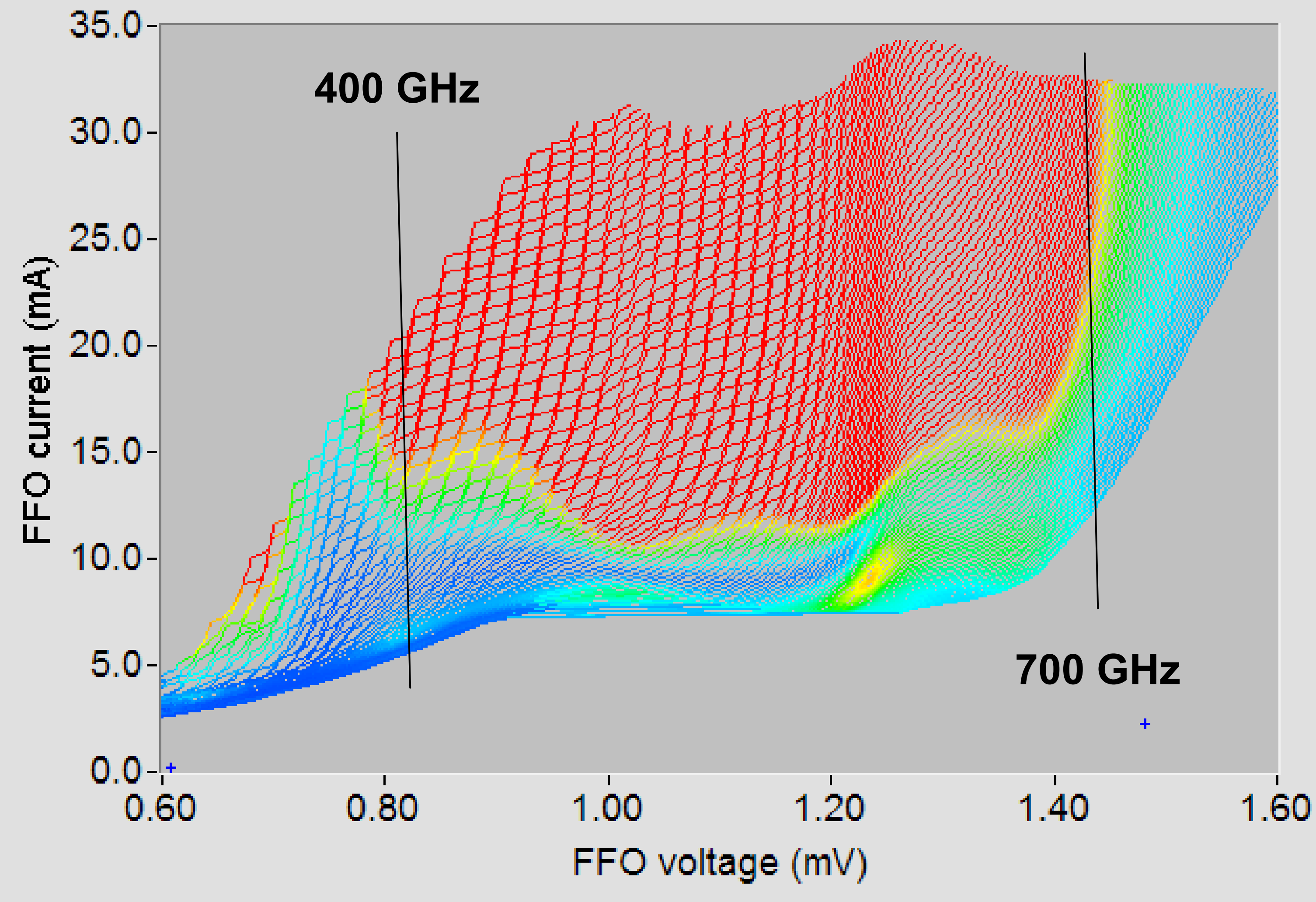

SIR Mixer Block with Shields

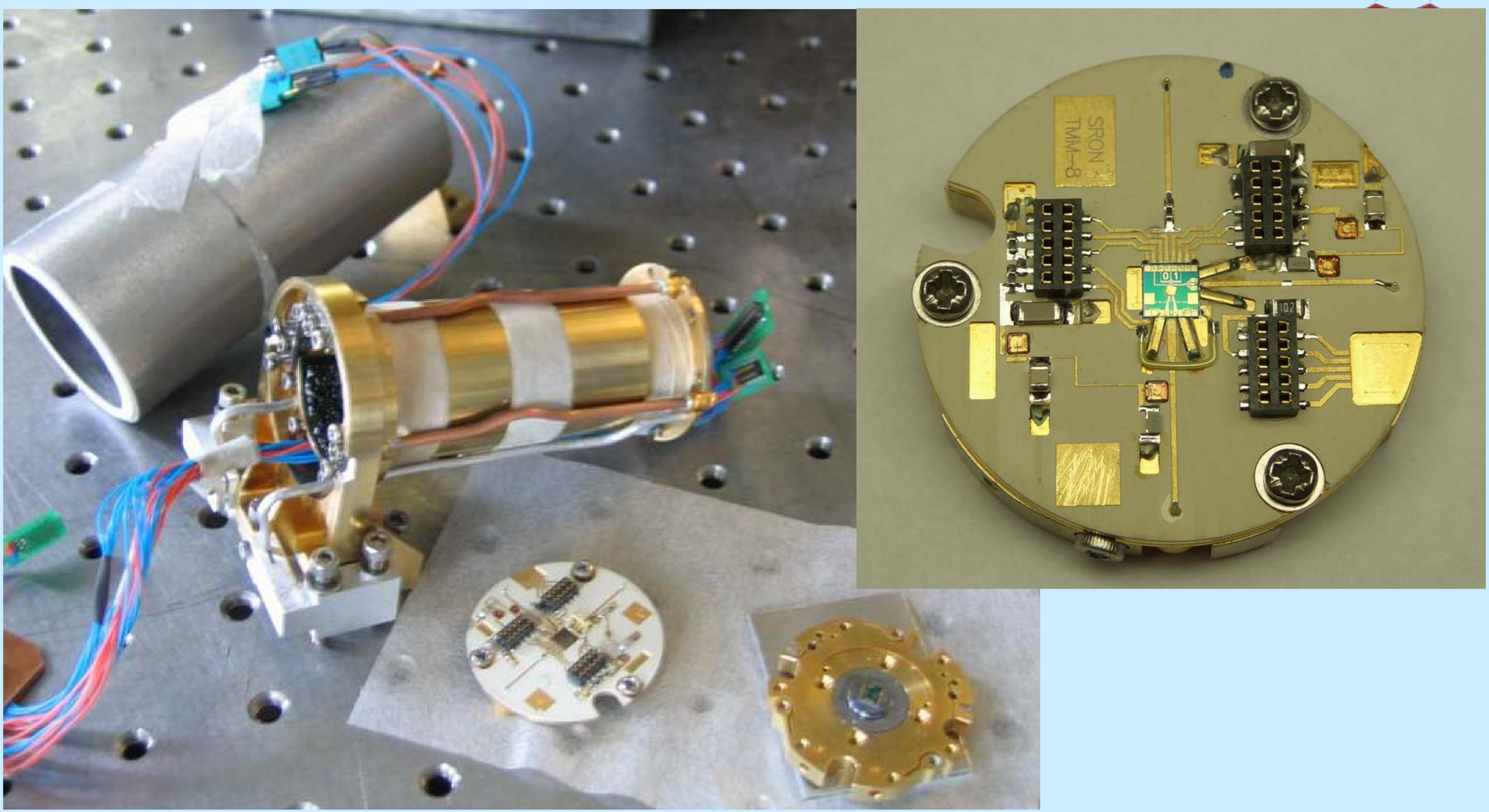

TELIS project

First test flight was in June 2008 (Terezina, Brazil). Unfortunately some cables got too rigid and the cryostat lost vacuum when the balloon passed the tropopause (temperature was almost -70ºC).

But before that our SIR works perfectly (almost 3 hours of flight!). Furthermore, all devices are OK after landing.

Next flight was successful with 12 hours February 2009 in Kiruna, Sweden

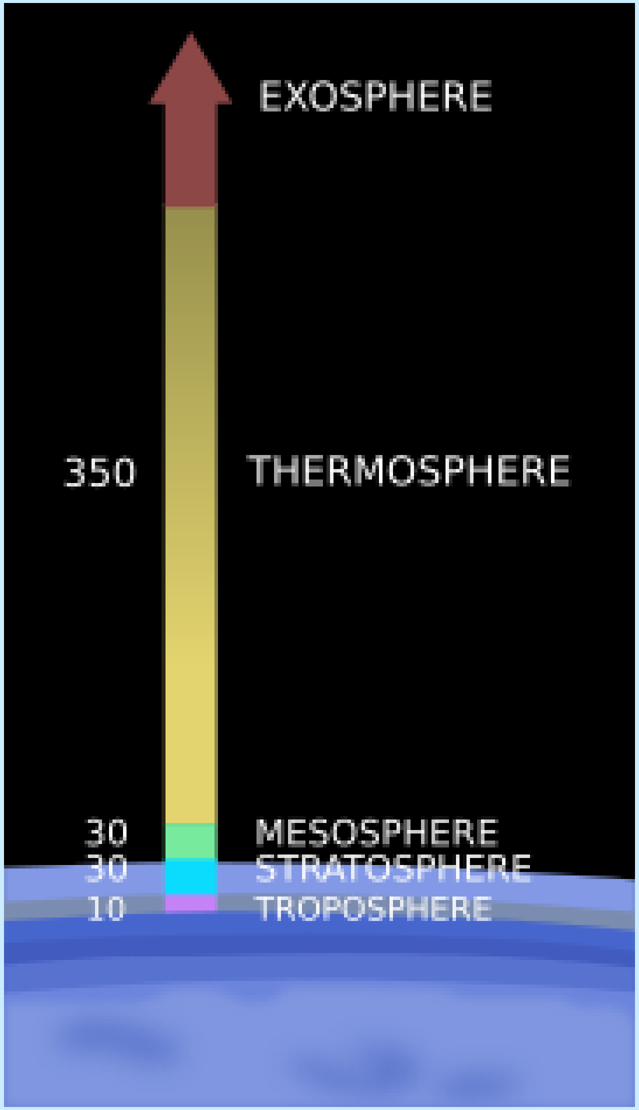

The **tropopause** is between the troposphere and the stratosphere.

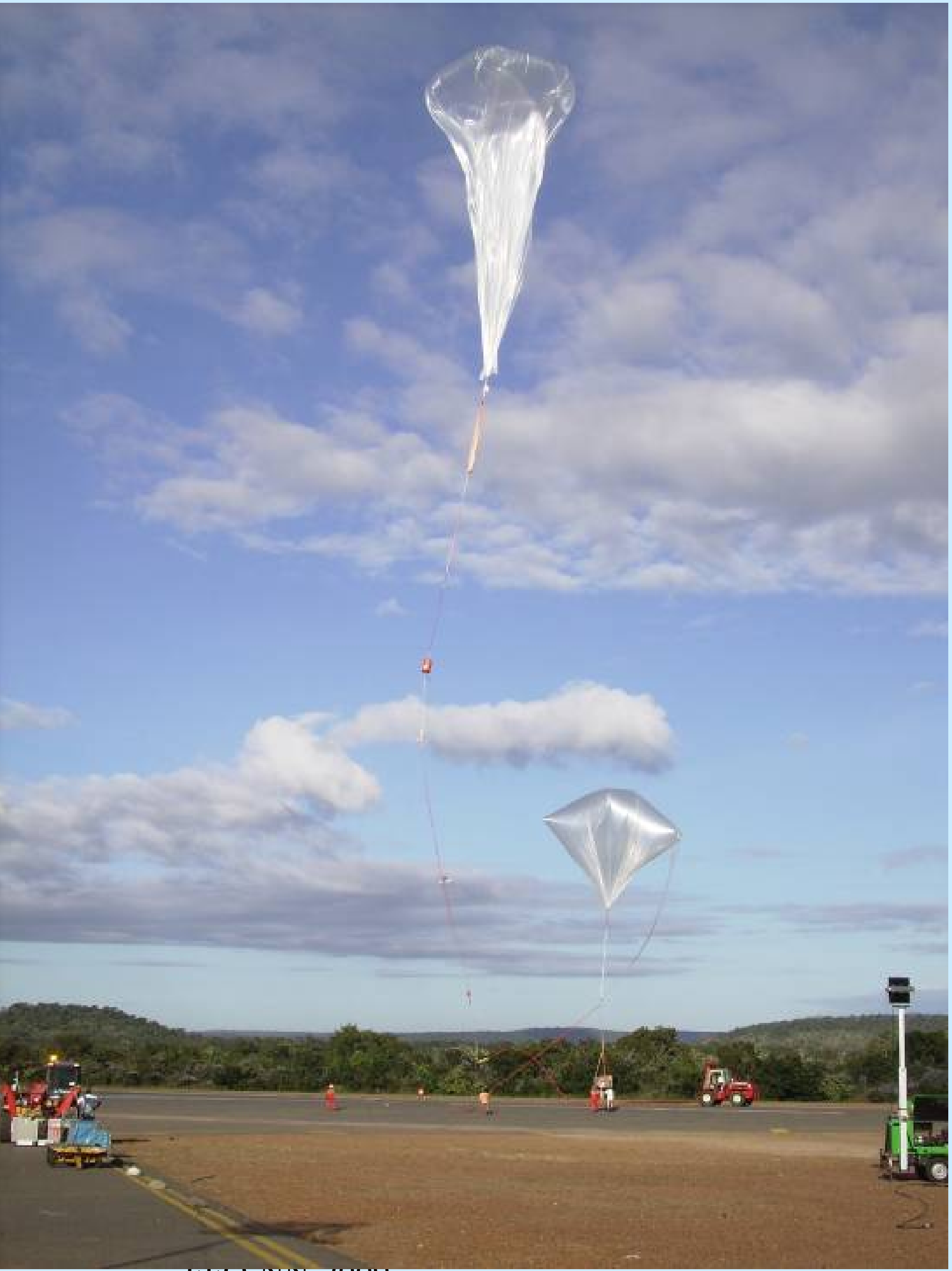

Esrange,

Kiruna,

Sweden

February 2009


HERCULES
CRAMO
CRAMO
4x4

ALMA –
The Atacama Large Millimeter Array

ALMA = Interferometer of 50+ antennas (12 m dia. each)
Working from 30 to 950 GHz
To be located in Northern Chile at 5000m altitude
Construction started, completion in 2012
Joint project Europe – North America – Japan

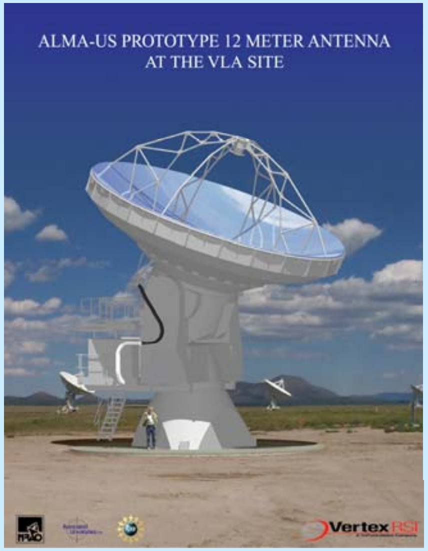

ESO’s ALMA project in Chile

ALMA at Chajnantor
(Courtesy NAOJ)

ESO PR Photo 14/01 (6 April 2001)

Spectral linewidth of the FFO

Central part of microcircuit used for FFO linewidth measurements

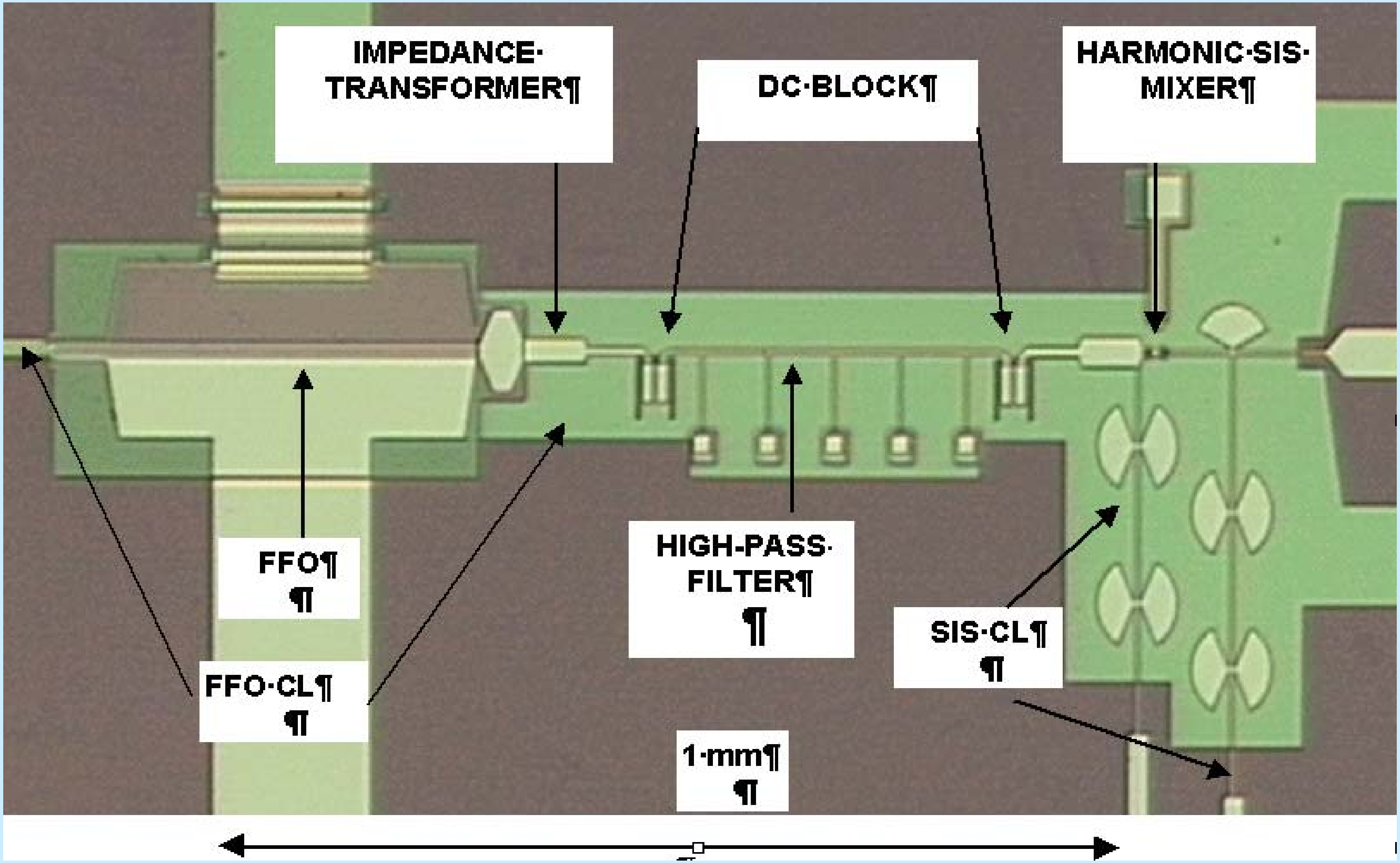

Theoretical linewidth of ideal FFO

(as of most other (all?) Josephson oscillators)

$\Delta\nu$ (FWHP, full width half power) of the *short* Josephson oscillator is determined by *internal* low frequency current fluctuations

$$\Delta\nu = \pi \frac{R_d^2}{\Phi_0^2} S_I(0)$$

with

$$S_I(0) = 2e\left\{I_{qp}\coth(\alpha) + 2I_s\coth(2\alpha)\right\}$$

and

$$\alpha = (eV_{dc})/(2\,k_B\,T_{eff})$$

Measurement of pair and quasiparticle current components on FFO *I-V* curves

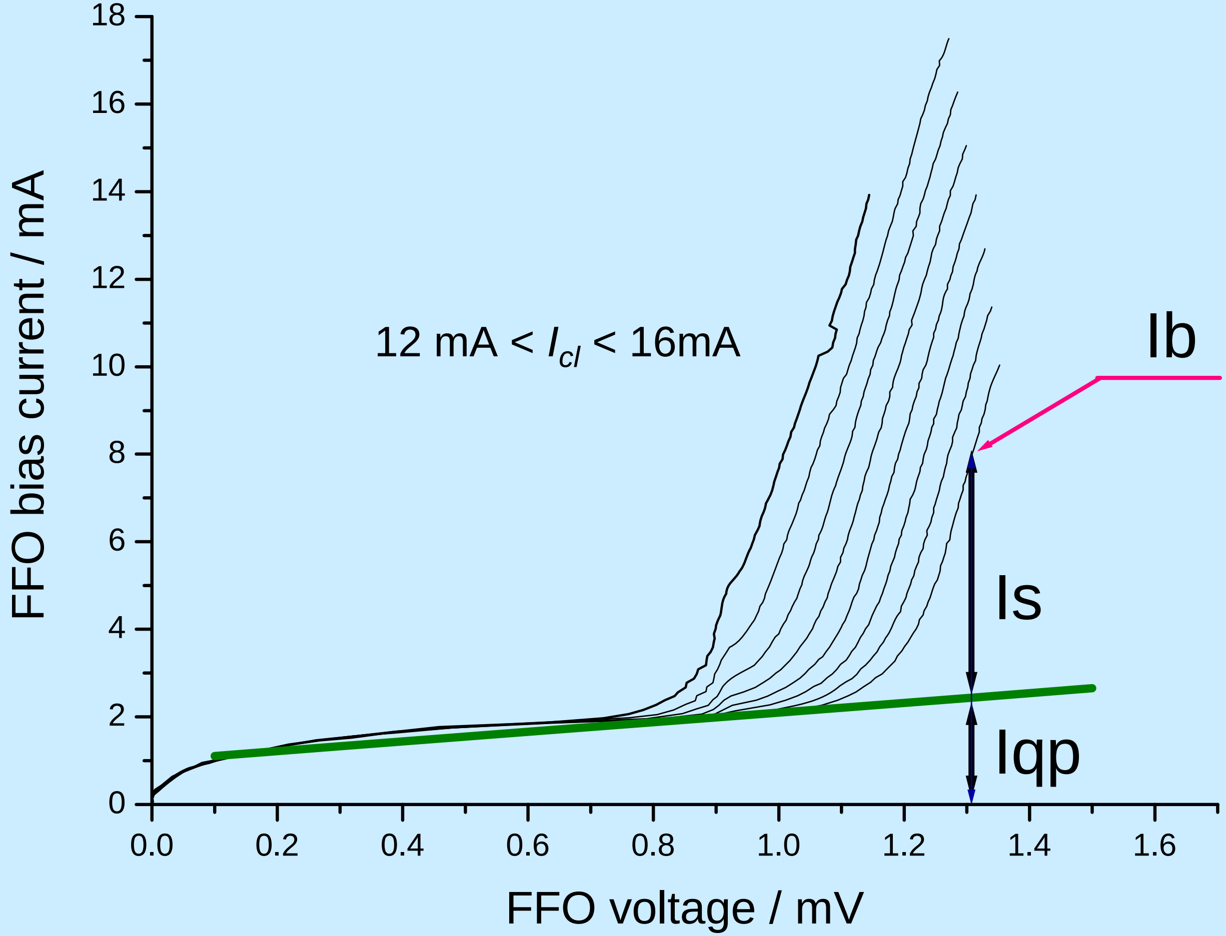

Experimental linewidth can be fitted with

$$\Delta \nu = \pi \frac{R_d^2}{\Phi_0^2} S_I(0)$$

Using a modified dynamic resistance $R_d^2 = (R_d^{'} + K \cdot R_d^{cl})^2$

where $R_d^{'} = \partial V / \partial I_b$ and $R_d^{cl} = \partial V / \partial I_{cl}$

are the derivative of the measured voltage, *V*, with respect to the DC bias current, I_b, and DC control line current, I_{cl}, respectively.

Note: No theoretical justification

Measure dynamic resistances from I-V curve

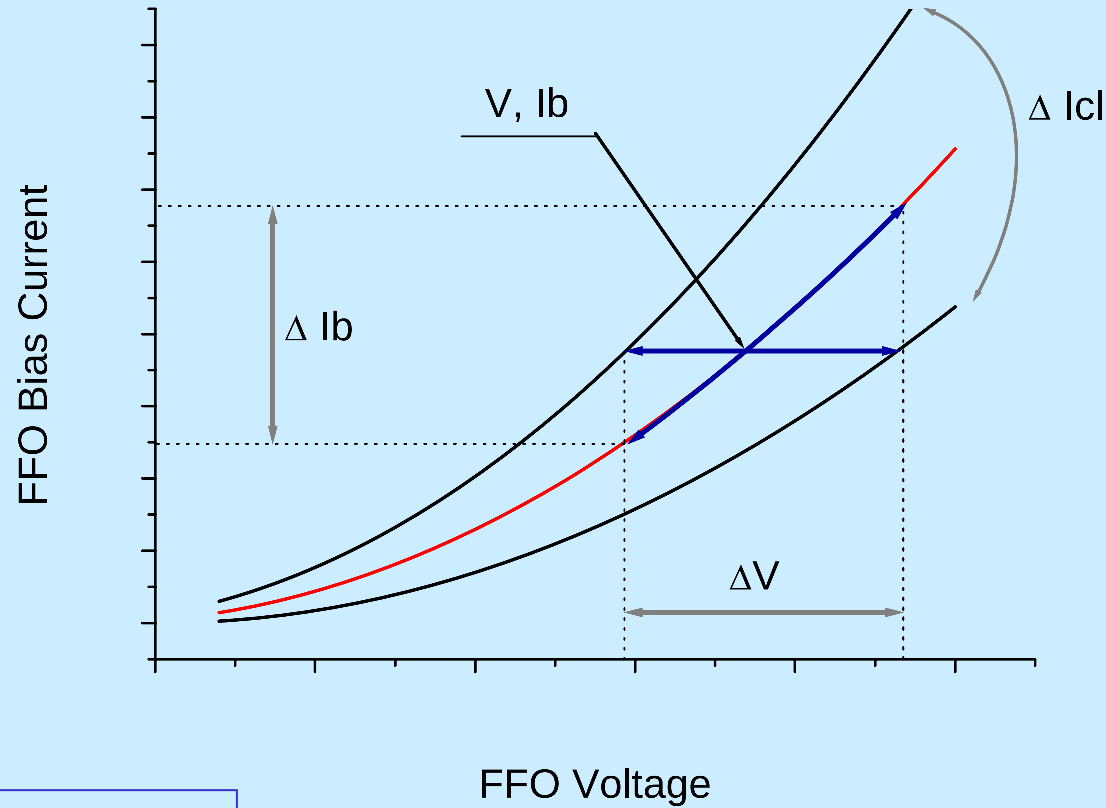

using

$$\Delta V \cong 500 \quad MHz$$

$$\sim 1 \ \mu V$$

we calculate:

$$R_d^{/} = \frac{\Delta V}{\Delta I_b}\bigg|_{I_{CL}} \quad \text{and} \quad \left(R_d^{CL}\right)^{/} = R_d^{CL} = \frac{\Delta V}{\Delta I_{CL}}\bigg|_{I_b}$$

FFO linewidth, example of spectrum

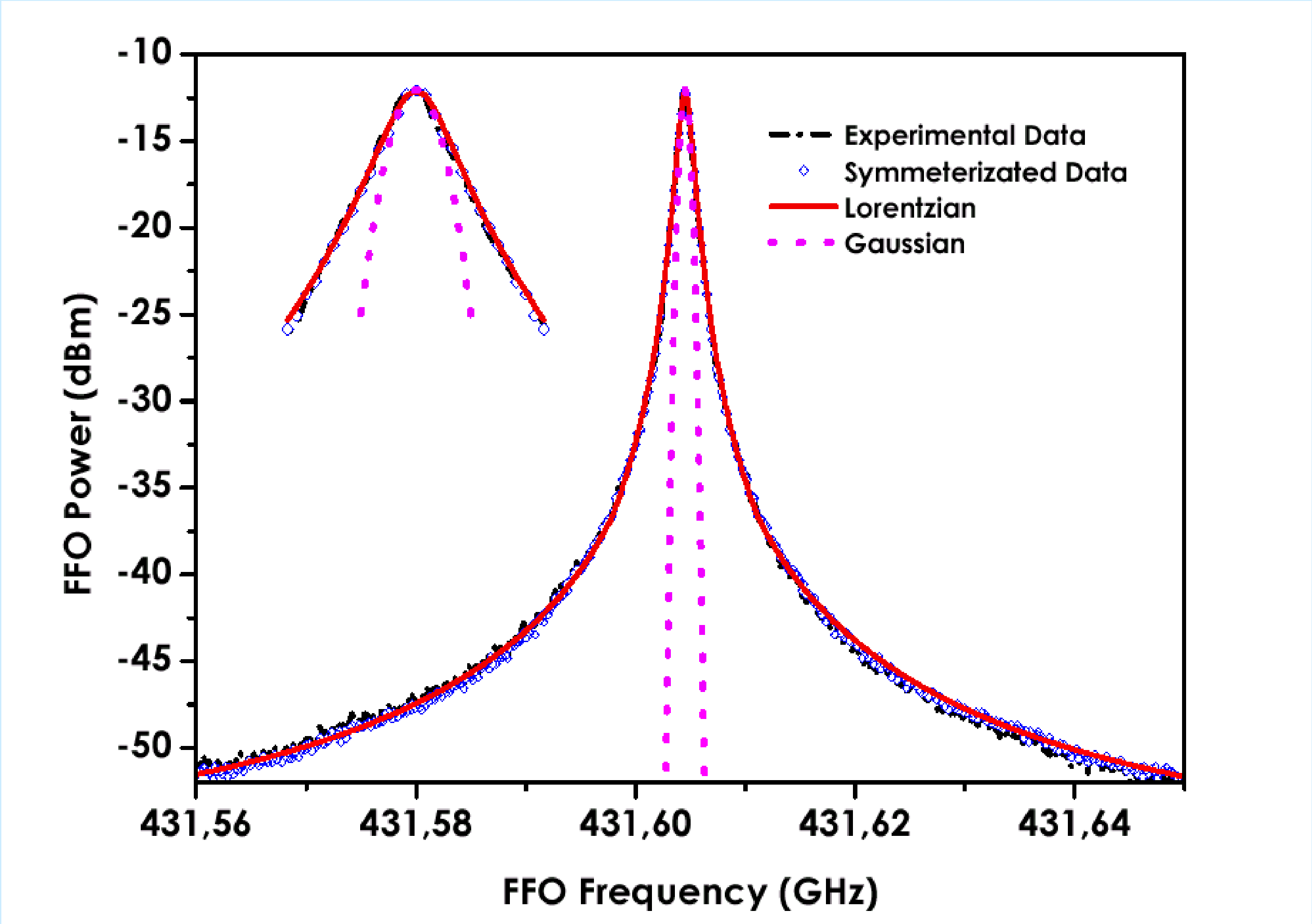

HD7 FFO linewidth vs differential resistance R'_d

Curves
1) K=0
2+3) K=2.9, fixed R_d^{CL}
Full curve: calculated for experimental parameters. E.g. for V_{dc}= 1 mV, I_{qp}=3 mA, I_s=7 mA, T_{eff} = 4.2 K
best fit: K=2.9 (ext)

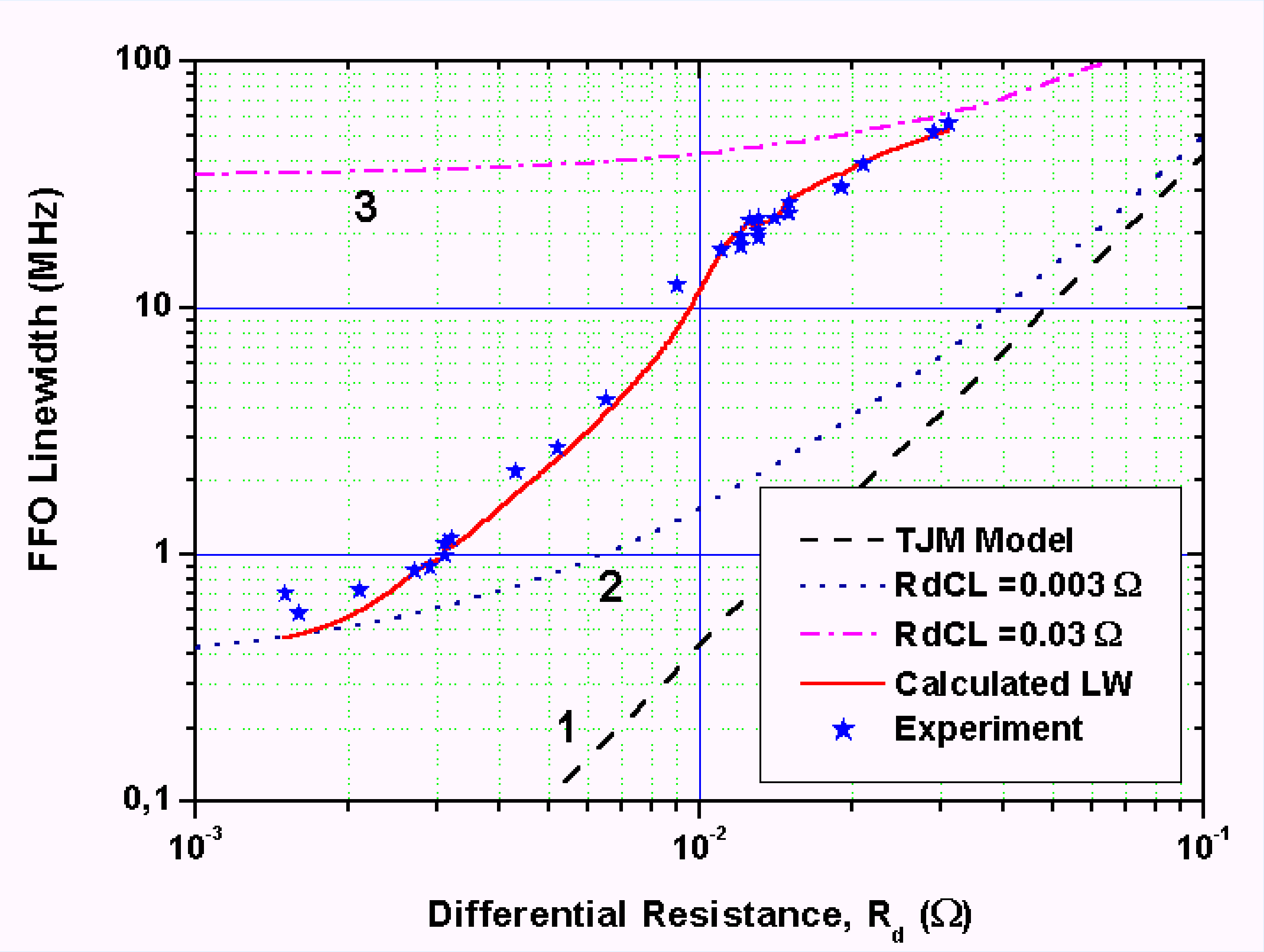

FFO spectra @ 707.45 GHz

Frequency locked; the free-running linewidth is δf_{AUT}=6.3MHz

and

phase-locked

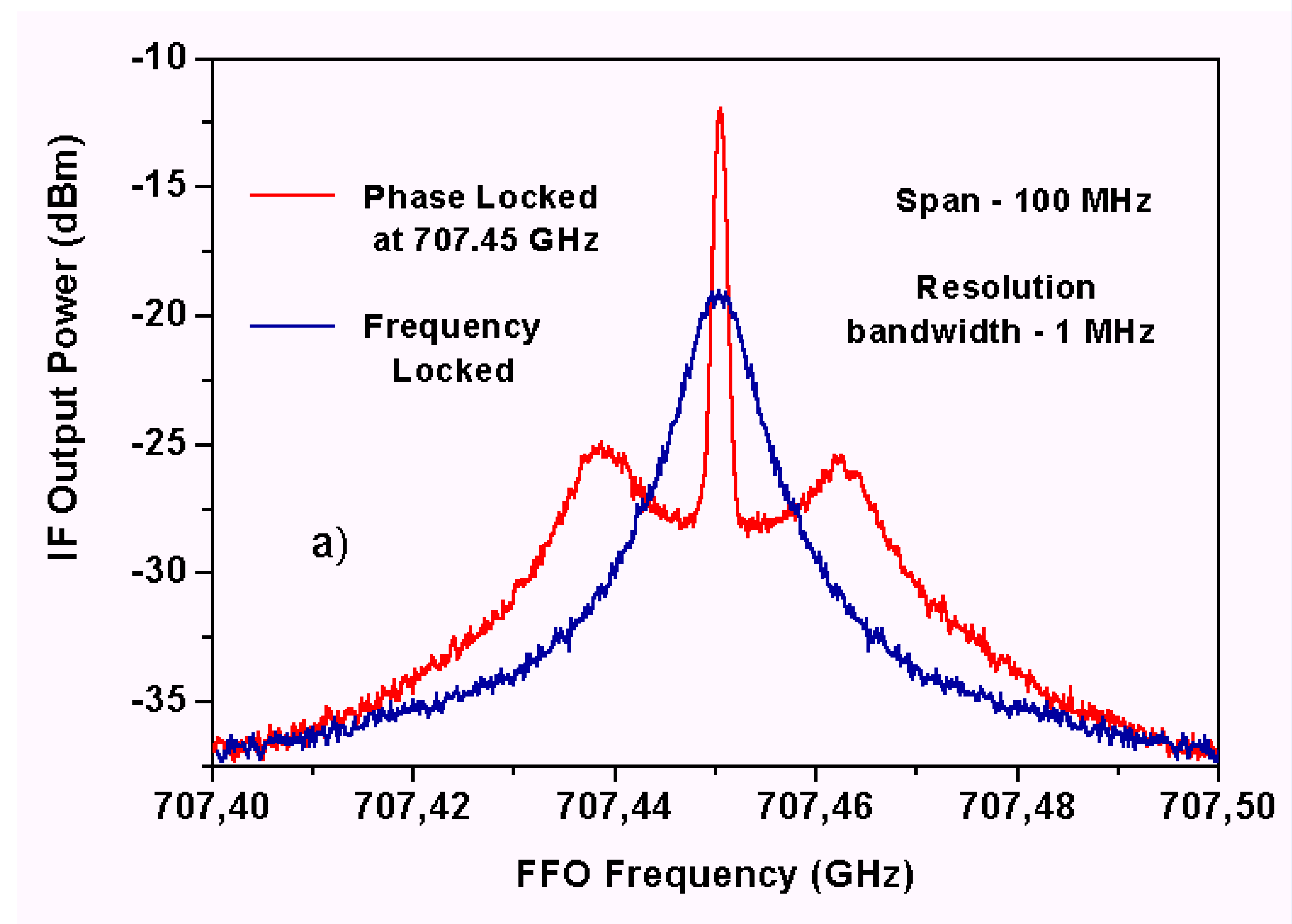

FFO spectrum @ 707.45 GHz
Phase-locked

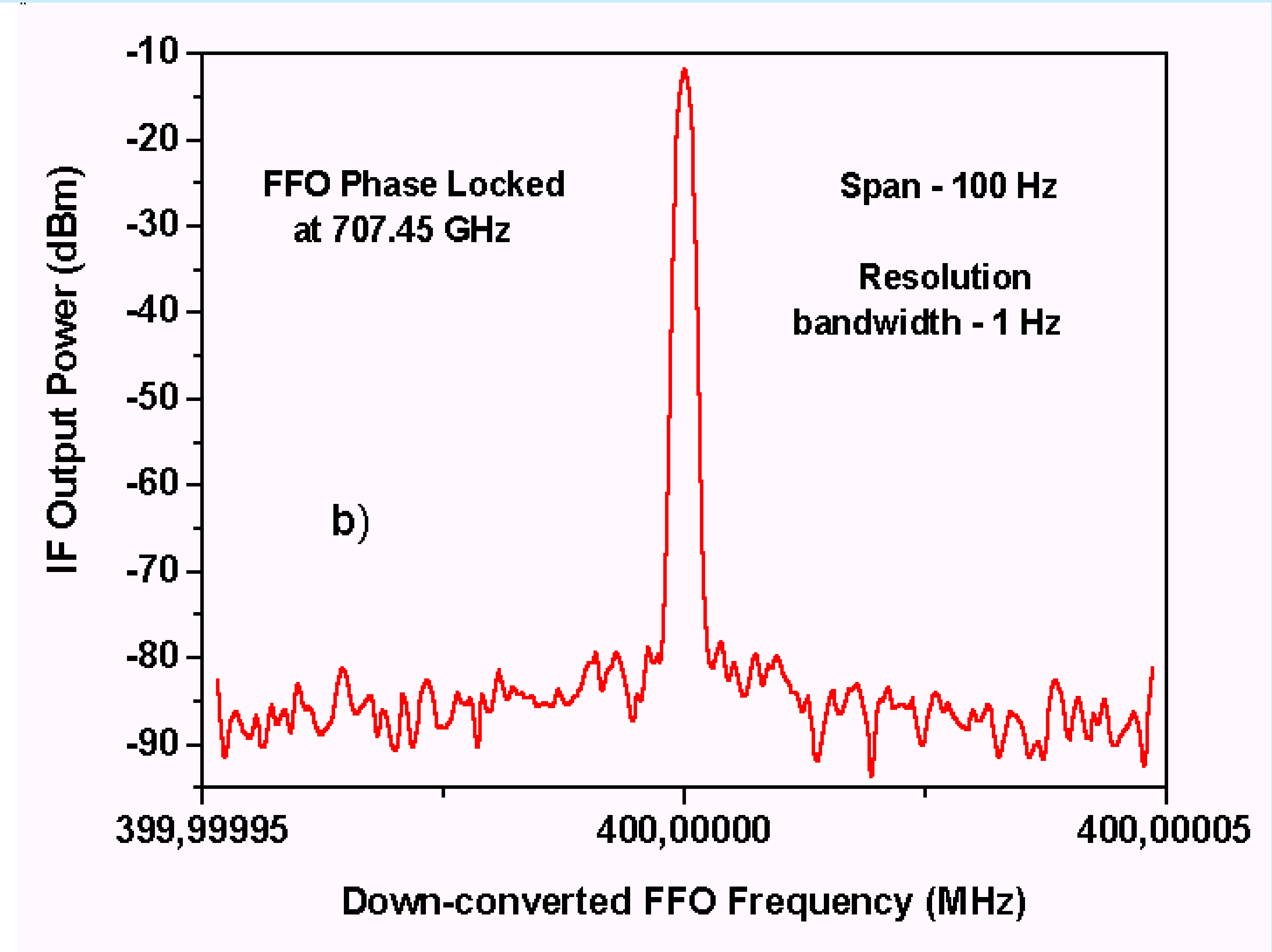

Experimental phase noise at 450 and 707 GHz

Note:

synthesizer noise multiplied by a factor n^2, should be added

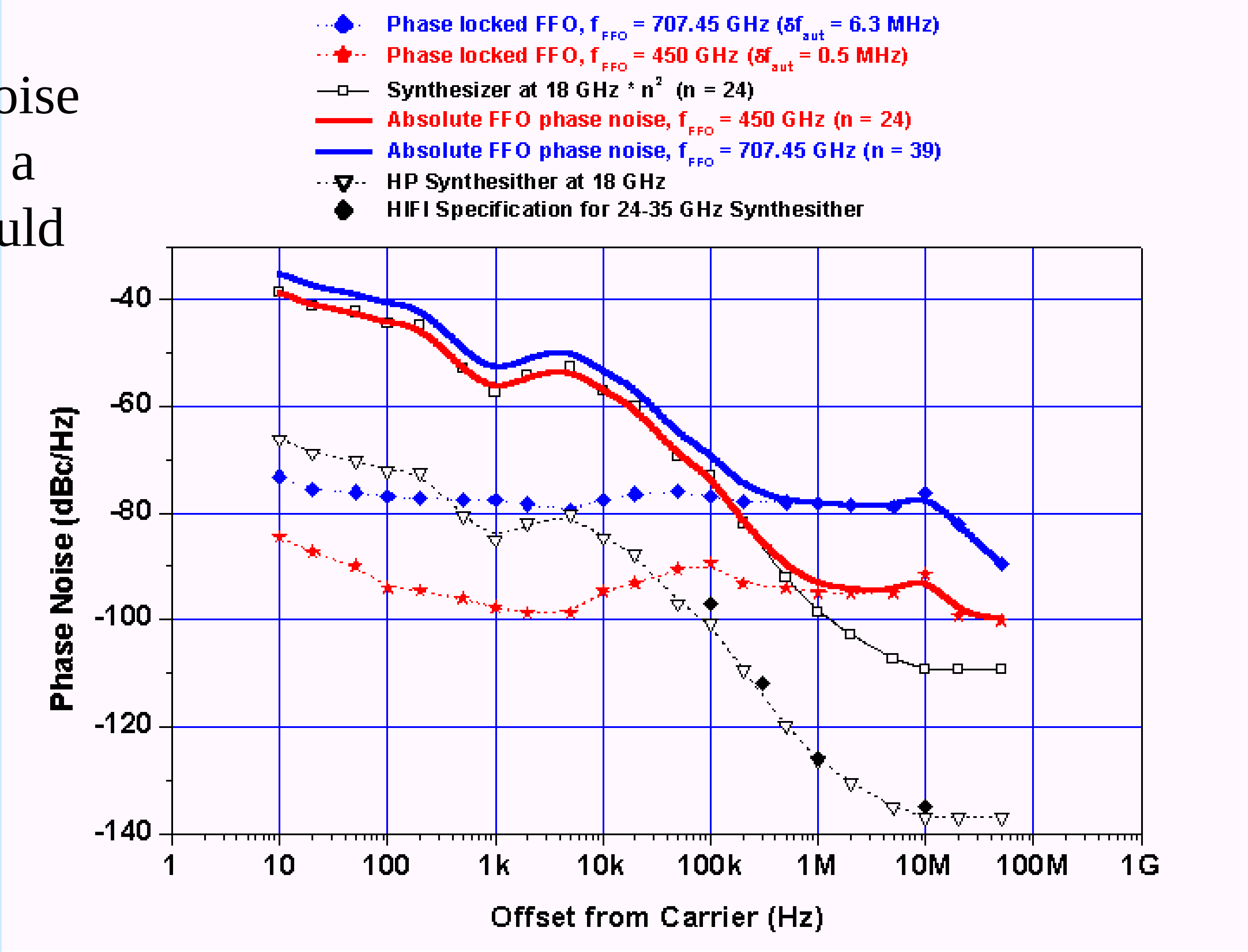

Mono-crystalline Sapphire Dielectric Resonator

Coupling loop →

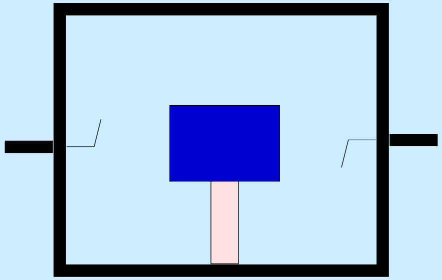

Cylindrical sapphire crystal in cylindrical copper cavity

Operated in high-order eigen-solutions to Maxwells equations so-called ”Whispering Gallery Modes” (WGM).

Sapphire axis →

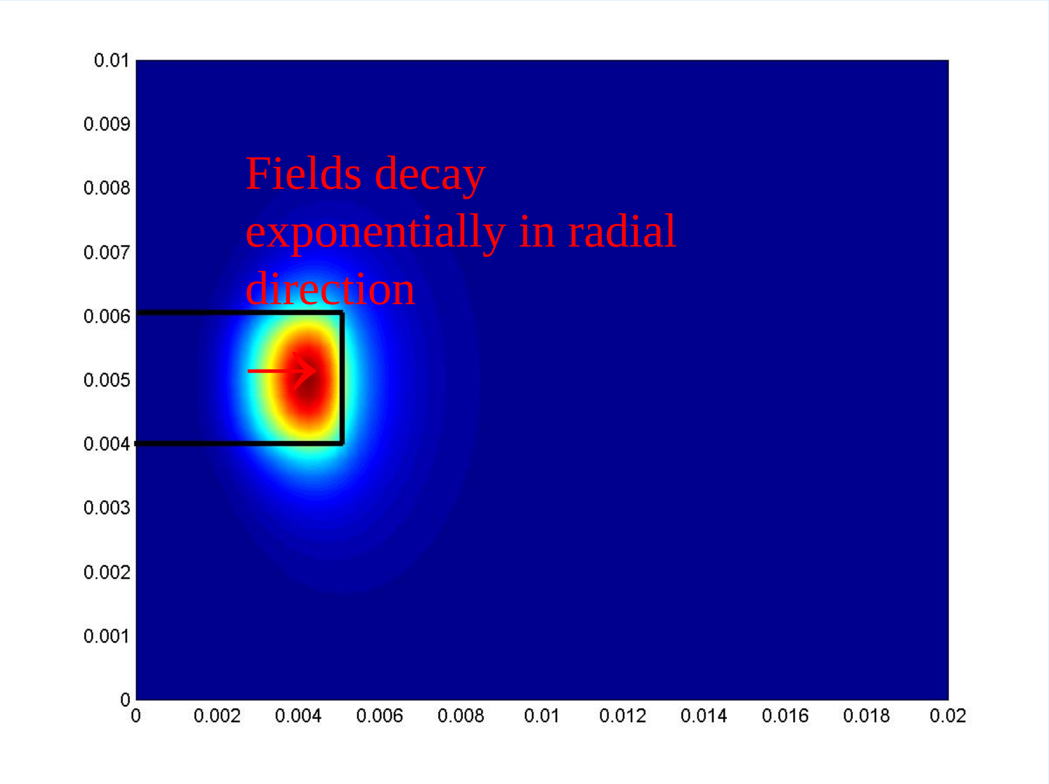

Whispering Gallery Mode Sapphire Oscillator

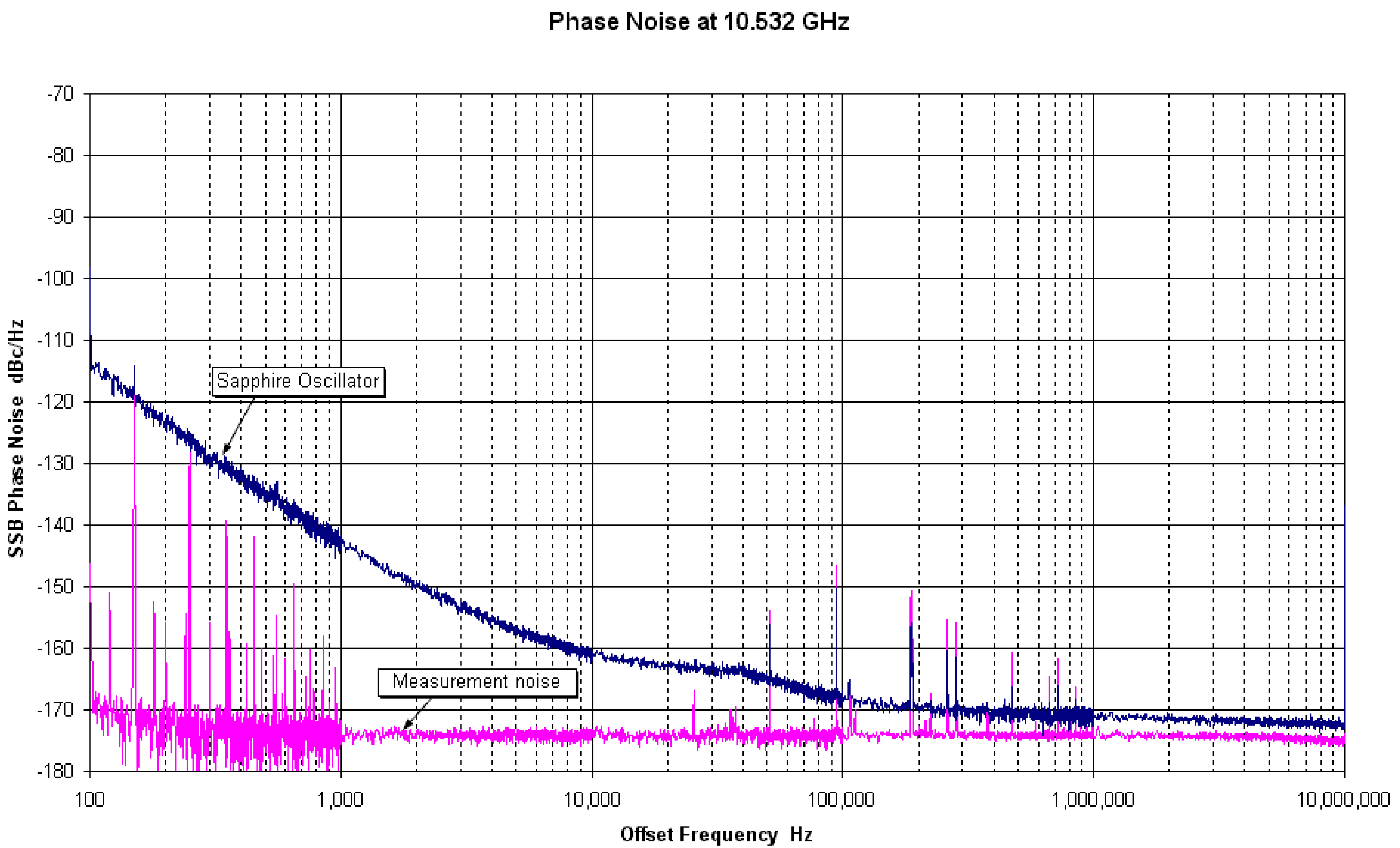

Simple theory for the linewidth of the FFO (or any Josephson oscillator)

Bare junction again (sine-Gordon)

The normalized magnetic field $\kappa_{1,2}$ enters as the boundary condition

$$\phi_x(0,t) = \kappa_1 \ \text{and} \ \phi_x(l,t) = \kappa_2, \tag{3}$$

specifying the magnetic field at the two ends of the junction. The total normalized current through the junction is

$$i = i_{ov} + i_{in} = w(\eta l + \kappa_2 - \kappa_1), \tag{4}$$

where $i_{ov} = \eta w l = (\int_0^l w(x)\eta(x)dx)$ is the normalized *overlap* current, $(\kappa_2 - \kappa_1)w = i_{in}$ is the *inline* part of the normalized junction current, and

$$\kappa = \frac{\kappa_1 + \kappa_2}{2} \tag{5}$$

is the normalized magnetic field, which we assume is applied in the plane of the junction and perpendicular to the x-direction. The overlap fraction of the junction current is [15]

$$\chi = \frac{i_{ov}}{i_{in} + i_{ov}}. \tag{6}$$

and the normalized I-V curve is

$$\omega = \omega(\eta, \kappa_1, \kappa_2) = \omega(i, \kappa), \tag{7}$$

Bare junction, dynamic resistances

We define two normalized dynamic resistances r_d and r_d^κ for the junction by

$$r_d = \frac{\partial \omega}{\partial i}, \quad r_d^\kappa = \frac{\partial \omega}{\partial \kappa} \frac{1}{w}, \qquad (8)$$

where the dynamic resistance r_d^κ is derived from a current $w\kappa$ equivalent to the magnetic field κ.

Until now everything relates to the ideal ("bare") junction where all partial derivatives are defined from Eq. (7) with i and κ as independent variables.

Measure dynamic resistances from I-V curve

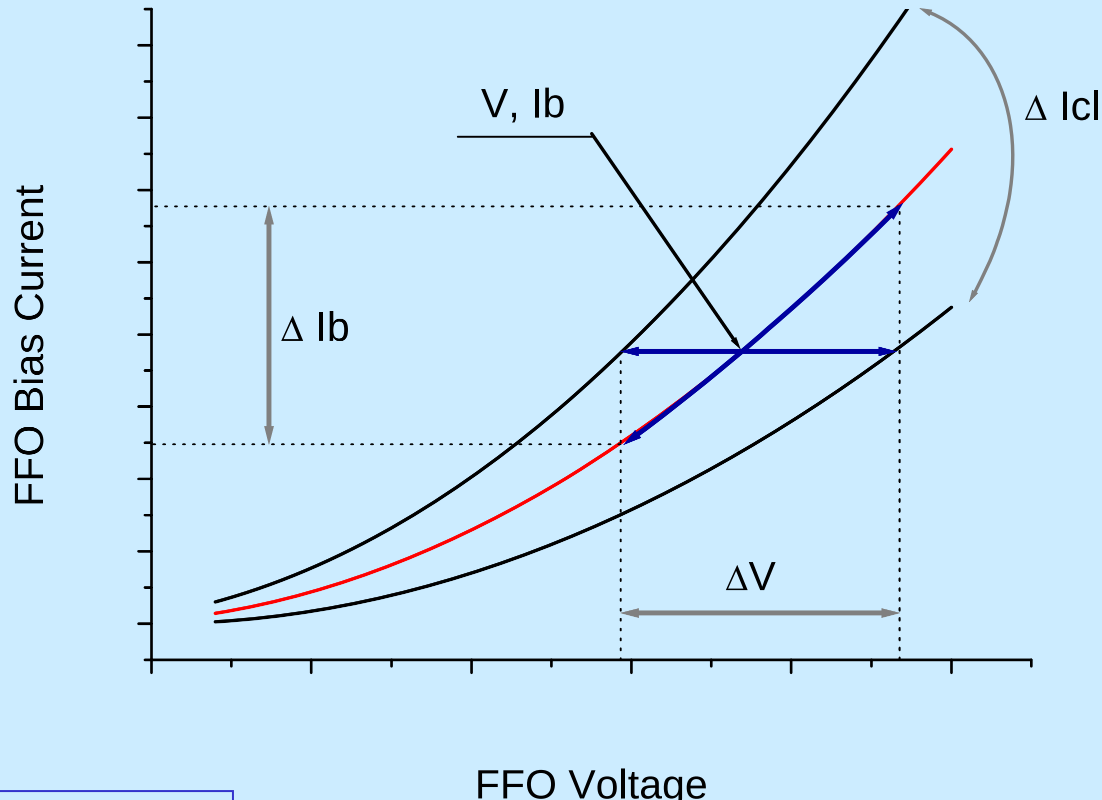

using

$$\Delta V \cong 500 \quad MHz$$

$$\sim 1 \quad \mu V$$

we calculate:

$$R_d^{/} = \left.\frac{\Delta V}{\Delta I_b}\right|_{I_{CL}} \quad \text{and} \quad \left(R_d^{CL}\right)^{/} = R_d^{CL} = \left.\frac{\Delta V}{\Delta I_{CL}}\right|_{I_b}$$

Long Josephson junction with magnetic field generated by the bias current

We now assume that the normalized magnetic field in the junction consists of two contributions, an externally applied field κ_{appl} proportional to a DC current, i_{cl} in a control line: $\kappa_{appl} = \beta i_{cl} \frac{1}{w}$, and a field proportional to the DC bias current through the junction i: $-\sigma i$. As exemplified below the latter may be due to asymmetry of the junction or the way the bias current is fed to the junction.

$$\kappa w = \kappa_{appl} w - \sigma i = \beta i_{cl} - \sigma i. \tag{9}$$

Here β and σ are dimensionless factors determined by junction geometry and bias conditions. Now the *measured* normalized I-V curve is

$$\omega = \omega(i, \beta i_{cl} - \sigma i), \tag{10}$$

and correspondingly the *measured* normalized dynamical resistance r'_d is given by :

$$r'_d = \left.\frac{d\omega}{di}\right|_{i_{cl}} = \frac{\partial \omega}{\partial i} + \frac{\partial \omega}{\partial \kappa}\frac{1}{w}(-\sigma) = r_d - \sigma r^{\kappa}_d. \tag{11}$$

Analog example:
Short JJ with coil

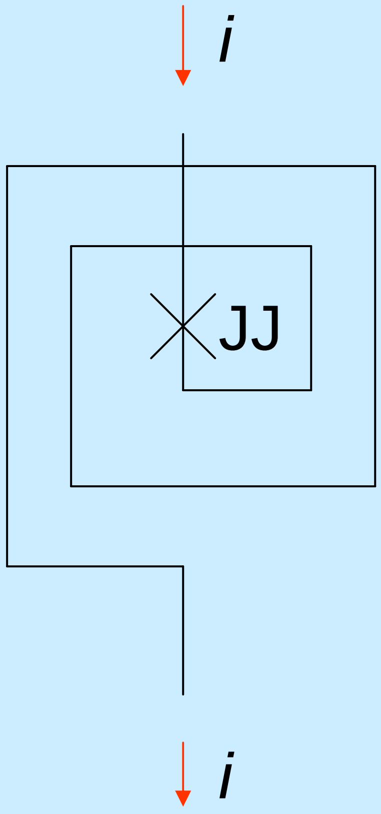

Magnetic field generated by the bias current

We define a normalized control line dynamical resistance r_d^{cl} given by

$$r_d^{cl} = \left.\frac{d\omega}{di_{cl}}\right|_i = \frac{\partial\omega}{\partial\kappa}\frac{1}{w}\beta = \beta r_d^{\kappa}. \qquad (12)$$

i.e. the *measured* control line dynamical resistance $(r_d^{cl})'$ is the same as before $(r_d^{cl})' = r_d^{cl}$. The normalized dynamic resistance, r_d, entering the linewidth expression Eq. (1) for the ideal junction is related to the *measured* dynamic resistances by

$$r_d = r_d' + \frac{\sigma}{\beta}(r_d^{cl})' = r_d' + K(r_d^{cl})', \qquad (13)$$

where we have defined the ratio between the two geometrical current factors, σ for the bias current and β for the control line current as $K = \frac{\sigma}{\beta}$. With the measured dynamical resistances introduced as in Eq. (13), and returning to unnormalized quantities, the linewidth expression Eq. (1) is replaced by

$$\Delta\nu = \pi\frac{(R_d' + KR_d^{cl})^2}{\phi_0^2}S_I(0), \qquad (14)$$

The derived equation contains just the empirical correction factor $(R_d' + KR_d^{cl})^2$ which was used by Koshelets et al. [12]

Construction of “measured” *I-V* curve from three “bare” junction *I-V* curves

Note:
$r_d' = 0$
and even
“back-bending”
is possible

The long lasting mistake

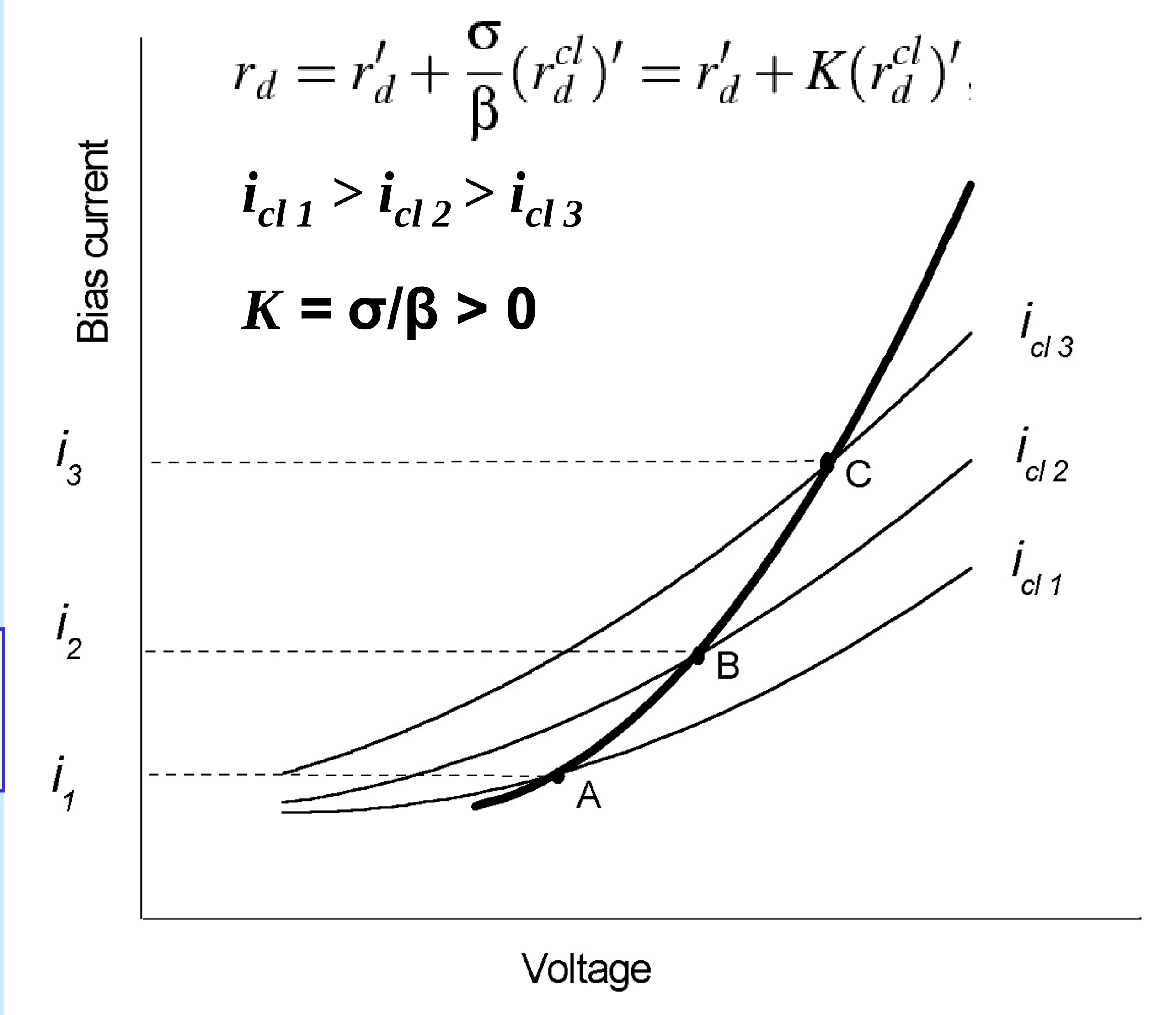

FFO with “unbiased tail”

The bias current generates a magnetic field that gives a steeper flux flow step

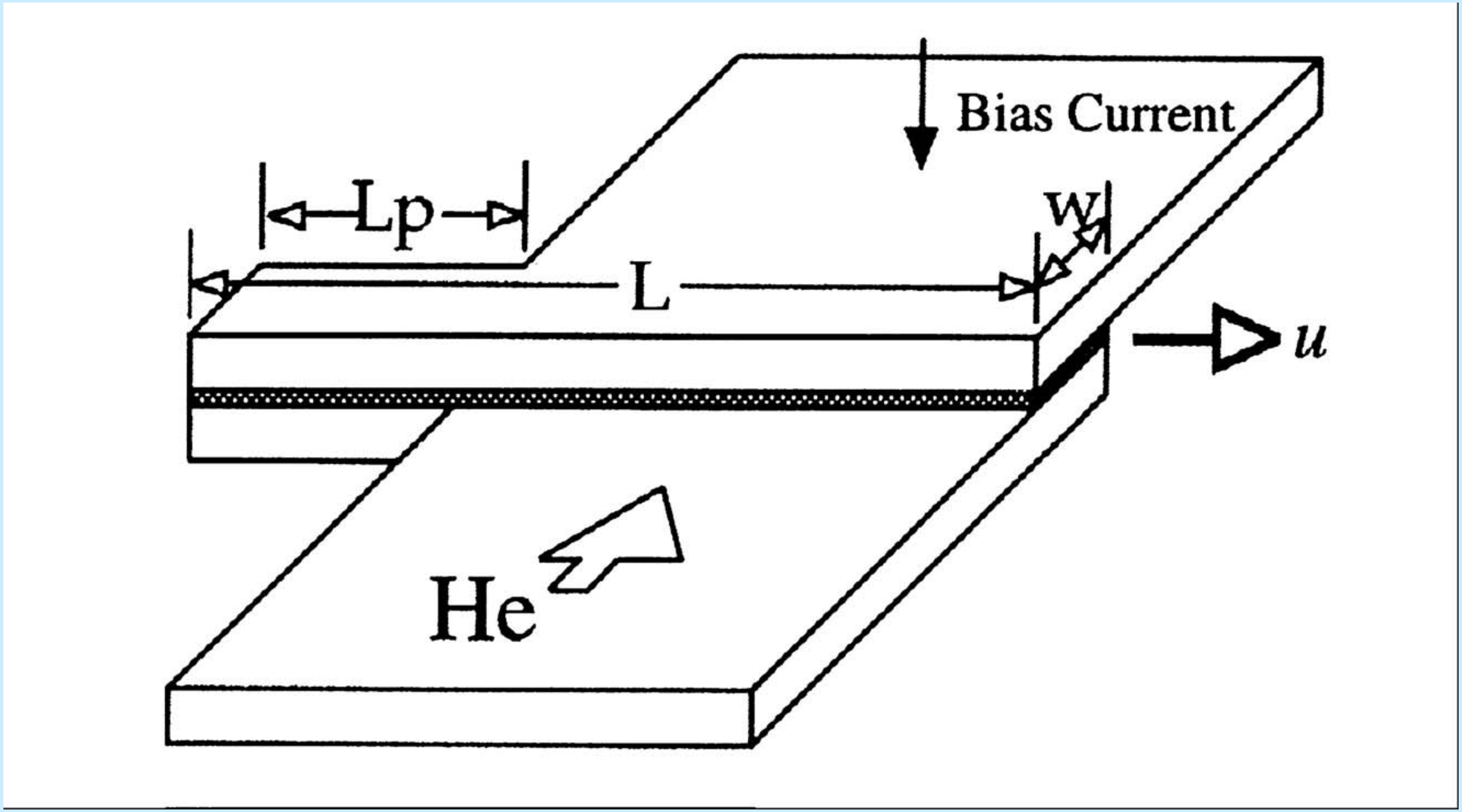

The three examples where we can clculate K

In general we can write

$$w\kappa_1 = \sigma_1 i + \beta_1 i_{cl}$$
$$w\kappa_2 = \sigma_2 i + \beta_2 i_{cl}$$
$$\eta w l = \sigma_3 i + \beta_3 i_{cl}.$$

From Eq. (4) we get

$$\sigma_2 - \sigma_1 + \sigma_3 = 1 \quad \text{and} \quad \beta_2 - \beta_1 + \beta_3 = 0.$$

$\sigma_2 - \sigma_1$ is just the inline fraction $1-\chi$ of the junction current and σ_3 is the overlap fraction χ. From Eq. (5) we get

$$\kappa = \frac{\sigma_1 + \sigma_2}{2}\, i + \frac{\beta_1 + \beta_2}{2}\, i_{cl}.$$

This should be identical to Eq. (9) therefore we have

$$-\sigma = \frac{\sigma_1 + \sigma_2}{2} \quad \text{and} \quad \beta = \frac{\beta_1 + \beta_2}{2}. \qquad (15)$$

It is clear that σ can be ascribed to an asymmetric feed of the junction. $K = \frac{\sigma}{\beta} = 1$ means that the bias current i and the control line current i_{cl} (if equal) produce the same magnetic field.

Examples no 1 and no 2

1) Pure overlap. If the bias current i is purely overlap ($\chi = 1$) there is no asymmetry in the bias current, therefore $\sigma = 0$ and $K = 0$.

2) Half inline. In the half inline case ($\chi = \frac{1}{2}$) there are two different cases. 2a) First the situation in Fig. 2. Simple considerations give

$$\sigma_2 \simeq \sigma_3 \simeq \frac{1}{2}, \quad \beta_2 = \beta_1 = \frac{1}{2}, \quad \text{and} \quad \sigma_1 \simeq \beta_3 \simeq 0,$$

or $\beta = \frac{1}{2}$ and $\sigma = \frac{1}{4}$ and therefore $K = \frac{1}{2}$. 2b) The other situation with half inline is shown in Fig. 3. Simple considerations now give

$$\sigma_2 \simeq \sigma_3 \simeq \beta_1 \simeq \beta_3 \simeq \frac{1}{2} \quad \text{and} \quad \sigma_1 \simeq \beta_2 \simeq 0,$$

or $\beta = \frac{1}{4}$ and $\sigma = \frac{1}{4}$ and therefore $K = 1$.

Example 2, Half-inline

Note:

Figures not to scale

The currents flow in the top or bottom of the superconducting films connecting to the “tunnel region”

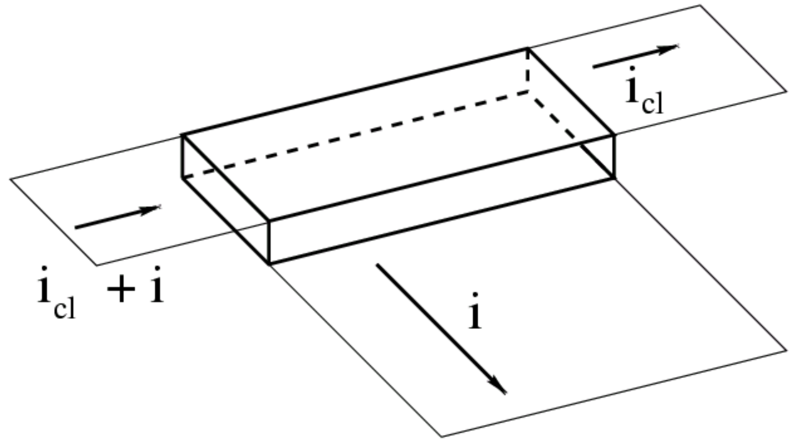

FIG. 2: Illustration of example 2a, $K = \frac{\sigma}{\beta} = \frac{1}{2}$, half inline, $\chi = \frac{1}{2}$.

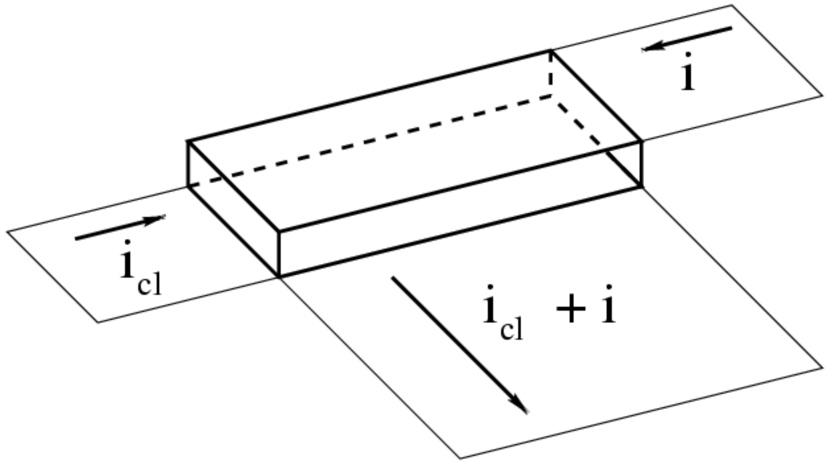

FIG. 3: Illustration of example 2b, $K = \frac{\sigma}{\beta} = 1$, half inline, $\chi = \frac{1}{2}$

Example no 3, pure inline

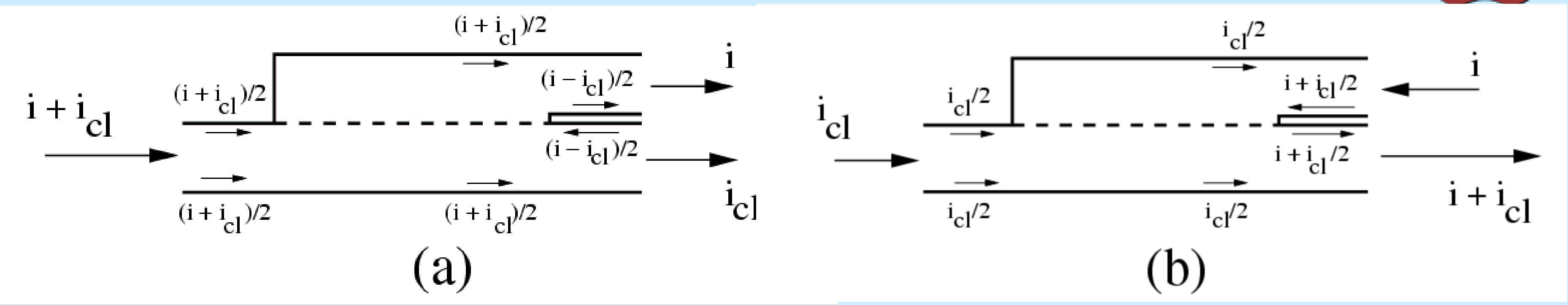

Fig.4

3) Pure inline. If the bias current is purely inline ($\chi = 0$) there are two cases to consider. Let the control line current i_{cl} flow in the bottom film. If the bias current i flows into one end of the junction from the bottom film and leaves the junction through the top film and the other end of the junction (Fig. 4a) there is no asymmetry in the current, $\beta = \frac{1}{2}$ therefore $\sigma = 0$ and $K = 0$. If the bias current i leaves the junction from the same end as it enters (Fig. 4b) the asymmetry in the current is $\sigma = \frac{1}{2}$, $\beta = \frac{1}{2}$ and therefore $K = 1$.

Sobolev's experimental proof of

$$\Delta \nu = \pi \frac{R_d^2}{\Phi_0^2} S_I(0)$$

Using a modified dynamic resistance $R_d^2 = (R_d^{'} + K \cdot R_d^{cl})^2$

where $R_d^{'} = \partial V / \partial I_b$ and $R_d^{cl} = \partial V / \partial I_{cl}$

are the derivative of the measured voltage, *V*, with respect to the DC bias current, I_b, and DC control line current, I_{cl}, respectively.

Note: No theoretical justification

Chip lay-out (HD6)

Arrows show directions for bias current (black) and control line current (green) with “standard” bias configuration

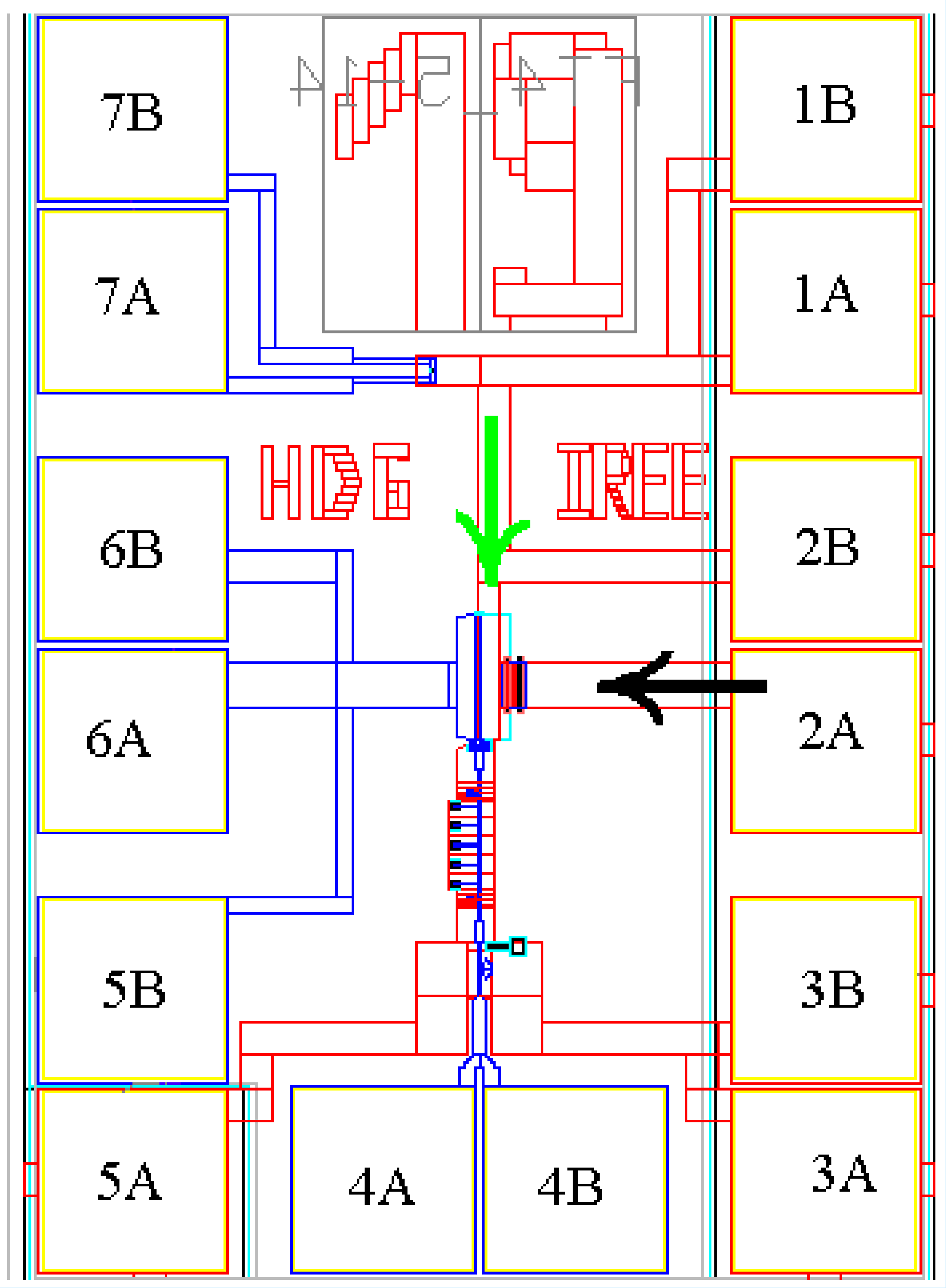

The 5 different bias configurations
(Chip HD6)

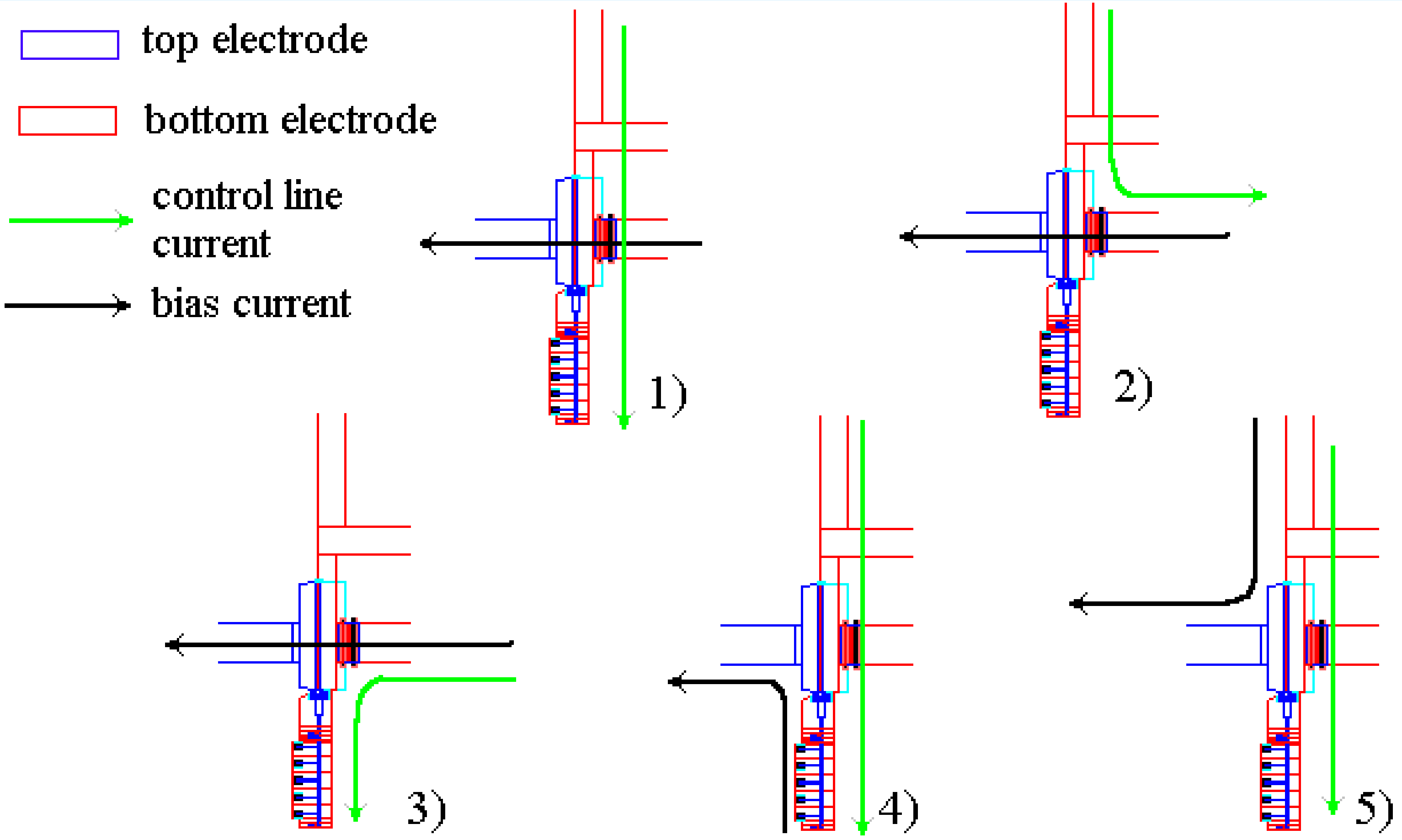

Bias configurations with *K* = +0.25 and *K*= -1.1

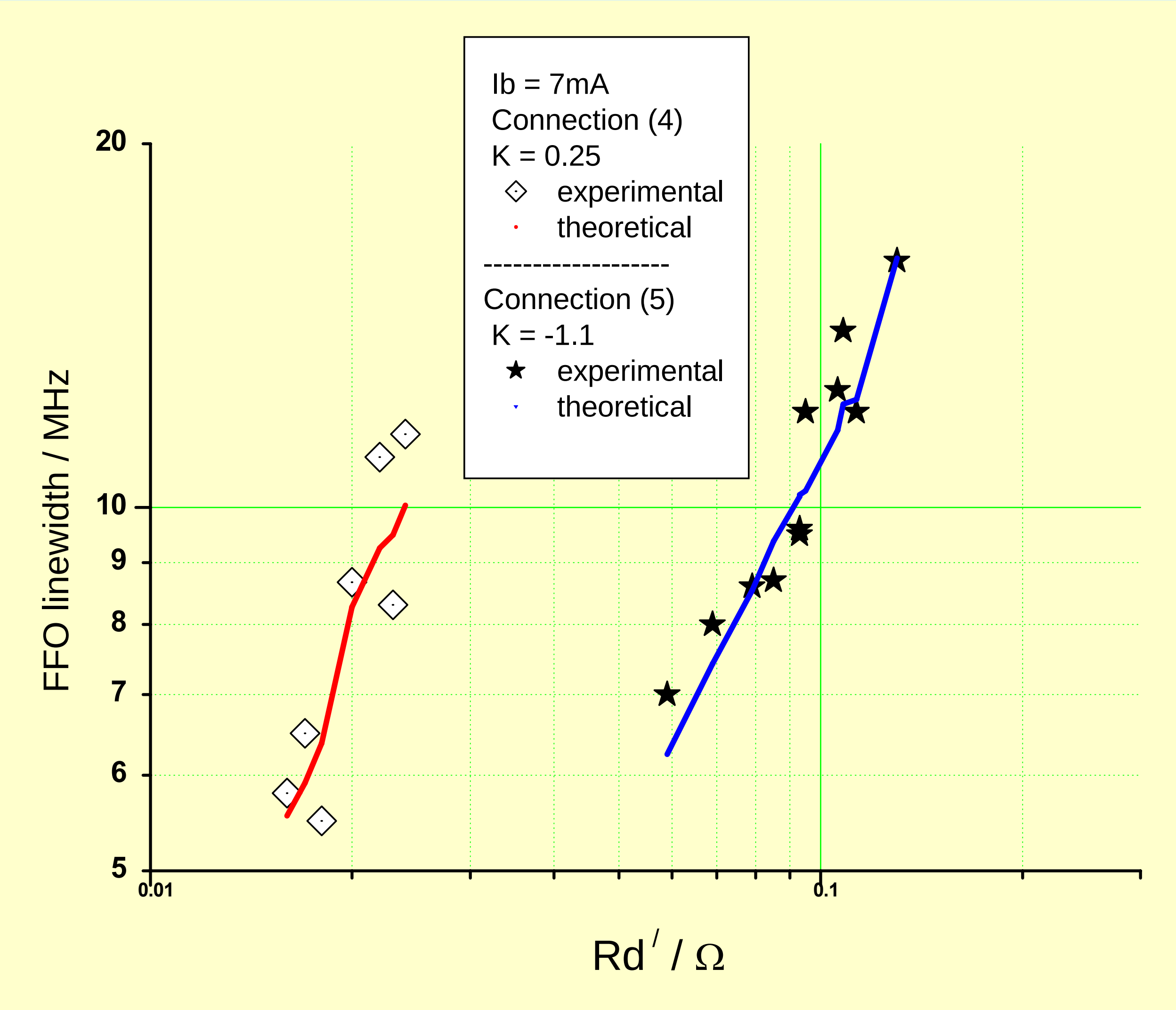

I_{CL}-*V* curves for different FFO bias configurations, *K*-values

Note:
factor 3 scales green curve to red curve

Factor 2.3 scales black curve to green curve

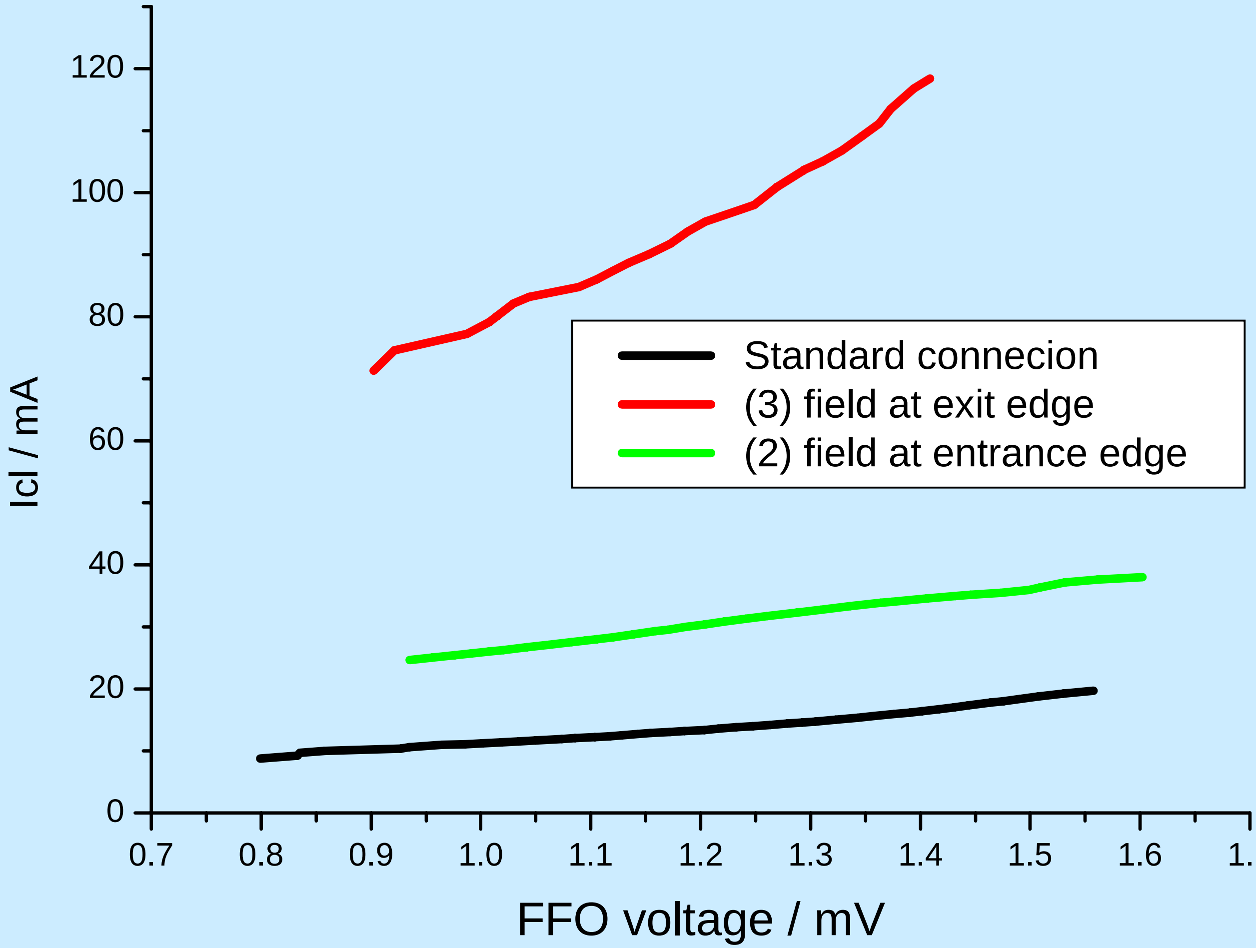

Conclusion and outlook

- Does the proposed simple theory for the linewidth of the FFO solve the long lasting discrepancy between theory and experiments?
- Do all Josephson oscillators - also those with additional magnetic bias - obey the short junction linewidth equation?
- The functional dependence on the two dynamic resistances seems to agree with recent measurements with different K-values, both positive and negative. Correlation. More experiments are needed!
- Accurate design rules for the FFO giving power and linewidth are required.
- Has anybody observed the parametric magnetic effect in short junctions with strong magnetic coupling (coil)? Make simulations! Is this effect important in the FFO?

Fin